THERMOMAGNETIC PHENOMENA IN MESOSCOPIC AND PARAMAGNETICALLY LIMITED SUPERCONDUCTORS

By

Mengling Hettinger

A DISSERTATION

Submitted to
Michigan State University
in partial fulfillment of the requirements
for the degree of

Physics - Doctor of Philosophy

2015

ABSTRACT

THERMOMAGNETIC PHENOMENA IN MESOSCOPIC AND PARAMAGNETICALLY LIMITED SUPERCONDUCTORS

By

Mengling Hettinger

The superconducting fluctuation effect, due to droplets of preformed Cooper pairs above the critical temperature T_c, governs the temperature dependence of kinetic coefficients in superconductors at the onset of the phase transition. The transverse thermoelectric response – Nernst effect – is particularly sensitive to the fluctuations, and the large Nernst signal found in the various superconducting materials has raised much debate on its connection to the origin of unconventional superconductivity. In this thesis, we present a systematic study of the electrical and thermomagnetic transport phenomena in mesoscopic and paramagnetically (Pauli) limited superconductors.

In the first chapter of this thesis we concentrate on the study of mesoscopic effects on transport in superconductors. We find that long-range phase coherence developing close to T_c triggers a great amplification of mesoscopic fluctuations due to strong pairing correlations. As a result, mesoscopic conductance fluctuations cease to be universal and exhibit pronounced dependence on temperature. Despite the lack of universality, in the sense of random matrix theory classification, we have discovered a different kind of universality in terms of temperature dependence of fluctuating characteristics. We find that mesoscopic fluctuations of conductivity, transversal thermoelectric coefficient and diamagnetic susceptibility consistently display the same scaling with temperature close to T_c. We connect our results to the existing experimental measurements of conductance fluctuations in superconducting films. Experimental verification of the temperature scaling and the overall magnitude of

the mesoscopic fluctuations of Nernst coefficient will provide a powerful tool for a better understanding of thermomagnetic transport phenomena in correlated systems.

In the second chapter of this thesis we examine the electrical and thermal transport anomalies in the ultra-thin superconducting films in an external in-plane magnetic field. We concentrate on the Clogston-Chandrasekhar phase transition, i.e., the destruction of superconductivity by a magnetic field by virtue of the Zeeman splitting. Near the quantum critical point of the supercooling line in the phase diagram, we discover highly non-monotonic magnetoresistance. The most remarkable feature of this effect is that fluctuation-induced transport is dominated by the virtual excitations rather than real preformed Cooper pairs. We also carefully study how spin-orbit scattering and other pair-breaking effects modify the fluctuation transport. In the strong spin-orbit scattering regime, we find that the scaling of the thermomagnetic coefficient is the same as conductivity within the classical region of transition, however they are drastically different near the quantum critical point. Even though we primarily focus on the conventional superconductors our result for the Nernst effect may have important implications to the other systems, such as iron-pnictides, and in particular to FeSe compound, which has comparable Zeeman and superconducting gaps.

ACKNOWLEDGMENTS

First and foremost, I would like to express my sincerest gratitude to my advisor, Dr. Alex Levchenko, who has been patient, supportive, encouraging, caring and understanding since the day I began working with him. His vast knowledge and skills in many areas in condensed matter physics guided me through the process of doing research and writing this thesis. The excellent research atmosphere he provided is simply the best one can possibly ask for.

I must thank all the physics and astronomy professors whom I have worked with and learned from over the past five years and whom I have received the time, energy and expertise from. My thesis committee guided me through all these years. I would like to give special thanks to professor Vladimir Zelevinsky, Carlo Piermarocchi, Norman Birge and Scott Pratt for being excellent teachers during my courses of study, and for providing insightful suggestions, constructive feedback and, thoughtful comments at all levels of my research projects.

I would never have been able to finish my thesis without the help from my great and cheerful friends and family. I owe a debt of gratitude for the constant support, concern, trust and love to my parents He Zhang, Feng Wang and Rita Murray, and my grandparents Rengsun Zhang and Yunfang Zhang. To my husband, Thomas Hettinger, thank you for listening to my endless complaints and concerns, offering me precious advices, supporting my decisions, and helping me unconditionally through this entire journey.

I want to thank all my friends who always be there cheering me up and stood by me through the good times and bad.

The research presented in this thesis was supported in part by National Science Foundation Grants No. DMR-1401908 and ECCS-1407875.

TABLE OF CONTENTS

LIST OF FIGURES

Chapter 1

Introduction

The study of fluctuation effects at the onset of the second order phase transition, which naturally emerged from the Landau's theory of the phase transformations [1], was instrumental in the development of statistical mechanics and modern condensed matter theory. The seemingly simple question – how accurately does the mean field theory describes the second order phase transitions – lead to the ideas of scaling, universality [2–6], and eventually to the development of the renormalization group [7]. In the context of superconductivity, fluctuations were first studied by Ginzburg [8]. In particular, he analyzed effects of fluctuations above the critical transition temperature, T_c, on the thermodynamic properties of superconductors and demonstrated that, in clean materials with ballistic transport, the fluctuation phenomena become important only in a very narrow temperature region near the transition. This result explained the great level of accuracy of the Bardeen-Cooper-Schrieffer (BCS) theory of superconductivity [9] (which in its essence is a mean field model) in application to various existing experiments of that time. Almost a decade later Aslamazov and Larkin [10], and independently Maki [11] and Thompson [12], realized that the fluctuation region in disordered superconducting films is determined by the resistance per unit square and could be much wider than that in bulk samples. Perhaps even more importantly they demonstrated that within microscopic BCS theory superconducting fluctuations, in fact, play a very important role in explaining temperature dependence of kinetic coefficients, such as conductivity. These authors discovered the phenomenon which nowadays is called the *paraconductivity effect* – the decrease of the resistance of a superconductor in the normal phase with lowering temperature towards the critical temperature. In a parallel vein this effect was observed in experiments by Glover [13]. Little [14], Langer and Ambegaokar [15], and McCumber and Halperin [16] showed that superconducting fluctuations associated with the phase of the superconducting order parameter, so called *phase slips*, are also required to explain the residual resistance in the superconducting phase. At very low temperatures, thermal activation of the phase slips is severely suppressed, however resistance may appear due to quantum phase slip tunneling [17].

Abrahams, Redi and Woo [18] demonstrated that fluctuation effects play an important role at the level of single particle properties, namely fluctuation-induced formation of superconducting droplets in the normal state leads to the depletion in the density of states that manifests as a pronounced zero-bias anomaly revealed by the tunneling experiments. The delicate interplay between paraconductivity and density-of-states effects is instrumental in explaining transport anomalies as observed in the granular superconductors. These early studies set the stage for the new and fruitful field of research that spanned over many decades and were recently summarized in the monograph by Larkin and Varlamov [19].

What makes superconducting fluctuations so pronounced in experiments and interesting from the theoretical point of view is their strong dependence on temperature, magnetic field, frequency of external drive parameter, etc. In practice these characteristic features allow one to separate fluctuations from the other competing effects contributing to transport, and use them to extract important information about the microscopic parameters of a material which are not accessible by other means of measurement. In theory, studying fluctuation effects advances our understanding of the underlying origin of superconductivity as a macroscopic quantum phenomenon. This becomes especially critical in the cases when this origin is in fact not completely known, like in the case of high-temperature cuprate superconductors or heavy-fermion superconductors. Furthermore, many ideas of the theory of superconducting fluctuations have been extensively used in other branches of condensed matter physics, e.g. in developing ideas of quantum criticality. For instance, superconducting fluctuations at zero temperature near the upper-critical field, H_{c2}, give perhaps the simplest example of a quantum critical metal.

A different kind of fluctuation effect that attracted tremendous attention over the span of last several decades is *mesoscopic* fluctuations [20–23]. This phenomenon occurs due to quantum mechanical interference between coherent electrons backscattering off random disorder potential. It manifests as completely reproducible oscillatory patterns of conductance as a function of magnetic field or the gate voltage with universal amplitude in the units of conductance quantum e^2/h. Since disorder substantially broadens the region of superconducting fluctuations, one may be intrigued by the question of whether there exists a parameter range within which superconducting fluctuations coexist with mesoscopic fluctuations, and what their interplay will give for observable quantities. In particular, one may want to investigate the ultimate fate of universality of conductance fluctuations in the presence of strong superconducting correlations. This set of questions defines the main theme of the present dissertation. Our focus in on thermomagnetic transport in mesoscopic superconductors. Thermomagnetic effects are difficult to measure and difficult to calculate theoretically. The mere difficulty of the problem makes it to be of fundamental importance.

In metals, thermomagnetic effects are usually small because of strong cancellation of currents generated by electronic excitations above and below the Fermi level – the electron-hole asymmetry is at the heart of the nonvanishing thermomagnetic response. Because of this compensation property, thermomagnetic effects are very sensitive to the characteristics of the electronic spectrum, presence of impurities, and peculiarities of scattering mechanisms. The inclusion of many-body interaction effects, such as electron-phonon renormalization, electron-electron scattering, drag effects, etc., adds a completely new level of complexity to the problem of calculating thermomagnetic kinetic coefficients. The observation that the collosal Nernst signal – the electric field, E_y, generated as a response to a transverse temperature gradient, $\nabla_x T$, in the presence of a perpendicular magnetic field, H – is mediated by superconducting fluctuations in the vicinity of transition triggered much interest to these transport phenomena.

On the technical side there is a well defined way how one can compute response functions based on the diagrammatic methods of many-body theory in condensed matter physics [24]. These methods are extremely powerful and, in the context of superconducting and mesoscopic fluctuation effects, can be reduced to the summation of certain classes of diagrams. The diagrammatic technique is especially suited for problems containing a small parameter when the whole treatment simplifies to the summation of ladder type diagrams. Importantly for our study, mesoscopic and superconducting fluctuations are controlled by the same parameter – inverse dimensionless conductance – which allows us to treat these effects on equal footing within the same formalism.

This dissertation is organized as follows. In Chapter-II we provide brief but yet sufficient introductory discussion for the foundations of mesoscopic physics of conductance fluctuations. We devote special attention to the mesoscopic effects in supeconducting systems.

After reviewing existing literature we place our work in the context of existing studies. Next we elaborate on the technical prerequisites and set the stage for the calculation of conductivity and transverse thermomagnetic power. We demonstrate that mesoscopic fluctuations proliferate in the presence of superconducting pairing correlations and that the universality of this phenomenon breaks down. We then relate our results to available experimental findings. In Chapter-III we concentrate on transport effects in thin superconducting films in the in-plane magnetic field. In such systems, superconductivity is limited either by orbital effects or by spin Zeeman effects. Depending on the film thickness and electron mean free path, one effect dominates the other and we consider both scenarios. In either case, the phase diagram in the field-temperature plane is interesting and we discuss fluctuation effects along the entire transition line including the most interesting quantum critical points. Despite certain similarity of the phase diagram, the underlying nature of fluctuation effects is conceptually different. The most remarkable feature of fluctuations in the Zeeman case (so called paramagnetically or equivalently Pauli limited superconductors) is that fluctuation-induced transport is mediated by *virtual* Cooper pairs in the quantum limit because of the Zeeman gap in the excitation spectrum at low temperatures. Chapter-III structurally is similar to Chapter-II. We review the history of studies on the subject of Pauli limited systems, discuss more recent tunneling results, and carry out calculation for electrical and thermomagnetic effects. Various technical aspects of this work are delegated to multiple appendices.

Chapter 2

Thermomagnetic transport in mesoscopic superconductors

2.1 Background and motivation

Universality of conductance fluctuations (UCF) is the hallmark of mesoscopic physics [20–23]. This phenomenon emerges from the quantum coherence of electron trajectories and is sensitive to changes in external magnetic field or gate voltage. At temperatures below the Thouless energy, $T < E_{Th}$, which is related to the inverse dwell time for an electron to diffuse across the sample $E_{Th} = D/L^2$, variance of conductance fluctuations saturates to the universal value of the order of conductance quantum, $\sim e^2/h$, as long as characteristic sample size L is smaller than dephasing length, $L < L_\phi$. Interaction effects in normal metals barely change the magnitude and universality of conductance fluctuations although they are crucially important in determining temperature dependence of dephasing effects, and in particular L_ϕ [25]. Robustness of UCF can be rooted to random matrix theory description of Wigner-Dyson statistics of electron energy levels in disordered conductors. Indeed, in the Landauer picture of transport across a mesoscopic sample, conductance is given by e^2/h times the number of single particle levels within the energy strip of the width of the Thouless energy. While the average number of such levels depends on the dimensionality, random matrix theory predicts that their fluctuations are universally of the order of one [26, 27].

When superconductivity is induced at the boundary of the mesoscopic sample via the proximity effect, UCF remain intact [28, 29]. The magnitude of oscillations changes only by a numerical factor of the order of unity, with a value depending on the underlying symmetry class [30–32]. Things get quantitatively different if superconducting correlations are induced at the bulk of the sample. Experimentally this is achieved by tuning superconducting systems to the vicinity of the critical temperature T_c or the superconductor-insulator transition. There exists compelling evidence from measurements such as those in two-dimensional granular arrays [33, 34], sub-micron scale superconducting cylinders [35], and quantum wires [36, 37], that mesoscopic oscillations could become anomalously large, sometimes reaching the level of $\sim 10^4 \times e^2/h$. These observations seemingly imply that the role of mesoscopic effects proliferate in the presence of superconducting correlations.

Theoretical studies devoted to various aspects of mesoscopic fluctuations in superconductors cover a diverse range of topics. These works include mesoscopic effects on the Josephson current [38–42], upper critical field [43,44], critical temperature [45], condensation energy and glassy phase transitions, [46,47] persistent currents [48–51], density of states, gap fluctuations and level statistics [52–56], and also some transport properties [57, 58]. In the recent years, measurements of the Nernst-Ettingshausen effect and the diamagnetic response in superconductors [59, 60], including high-T_c [61–69] and heavy-fermion systems [70–72], attracted tremendous attention and triggered a flood of theoretical works [73–83]. Our motivation is to study mesoscopic effects on the thermomagnetic transport in superconductors at the onset of T_c where pairing correlations due to preformed Cooper pairs are profoundly important. We find that in a parametrically wide temperature region, $g^{-1} < (T - T_c)/T_c \ll 1$, where g is the dimensionless conductance, amplitude of mesoscopic fluctuations in the diagonal component of the conductivity tensor σ_{xx} and transversal component of the thermomagnetic tensor α_{xy} become parametrically bigger than their bare values.

2.2 Foundations of UCF

In the multiple scattering diffusive regime, the quantum mechanical interference effects associated with coherent backscattering on impurities modify the average value of electrical conductivity. Similarly, correlation functions of the single-particle density of states are affected by the same coherence effect. In what follows, we discuss the second moment of these physical quantities which will lead us to the universality of conductance fluctuations.

The point of departure is the Einstein formula (throughout the text we use unites $\hbar = k_B = 1$)

$$\sigma_{\alpha\beta}(\varepsilon) = 2e^2\nu_d(\varepsilon)D_{\alpha\beta} \tag{2.1}$$

which relates conductivity $\sigma_{\alpha\beta}$ to the diffusion constant $D_{\alpha\beta}$ and density of states ν_d. We introduce the mean for conductivity $\bar{\sigma}$ and sample specific variance $\delta\sigma = \sigma - \bar{\sigma}$. Then the product

$$\langle\delta\sigma(\varepsilon)_{\alpha\beta}\delta\sigma_{\gamma\delta}(\varepsilon')\rangle = \sigma_0^2\left(\delta_{\alpha\beta}\delta_{\gamma\delta}\frac{\langle\delta\nu_d(\varepsilon)\delta\nu_d(\varepsilon')\rangle}{\nu_0^2} + \frac{\langle\delta D_{\alpha\beta}(\varepsilon)\delta D_{\gamma\delta}(\varepsilon')\rangle}{D^2}\right) \tag{2.2}$$

contains two contributions related to the density of states fluctuations and the diffusion coefficient fluctuations, while the cross-correlation between ν and D is absent. Here ν_0, D, and

σ_0 are bare disorder-averaged density of states, diffusion constant, and Drude conductivity respectively, while angular brackets $\langle\ldots\rangle$ stand for the disorder average of the irreducible correlation function. These correlation functions can be computed by using a conventional Diffuson-Cooperon diagrammatic technique [20–23]. The total conductivity fluctuation can be written in the form

$$\langle\delta\sigma_{\alpha\beta}(\varepsilon)\delta\sigma_{\gamma\delta}(\varepsilon')\rangle = \sigma_0^2\left[\delta_{\alpha\beta}\delta_{\gamma\delta}K_\nu(\varepsilon-\varepsilon') + (\delta_{\alpha\gamma}\delta_{\beta\delta}+\delta_{\alpha\delta}\delta_{\beta\gamma})K_D(\varepsilon-\varepsilon')\right], \tag{2.3}$$

$$K_\nu(\omega) = \frac{\langle\delta\nu_d(\varepsilon)\delta\nu_d(\varepsilon')\rangle}{\nu_0^2} = \frac{\delta^2}{2\beta\pi^2}\sum_q \mathrm{Re}\left(\frac{1}{Dq^2-i\omega}\right)^2, \tag{2.4}$$

$$K_D(\omega) = \frac{\langle\delta D(\varepsilon)\delta D(\varepsilon')\rangle}{D^2} = \frac{\delta^2}{2\beta\pi^2}\sum_q \frac{1}{[(Dq^2)^2+\omega^2]}, \tag{2.5}$$

where $\omega = \varepsilon - \varepsilon'$, $\delta = 1/\nu_d L^d$ is the mean level spacing and coefficient β captures the symmetry class. For the time reversal invariant system $\beta = 1$ (orthogonal ensemble), while $\beta = 2$ if it is not (unitary ensemble). To translate conductivity fluctuations into the conductance fluctuations at finite temperature one uses $g = \sigma L^{d-2}$ (assuming cubic conductor of size L) and $g(T) = \int g(\varepsilon)\partial_\varepsilon f d\varepsilon$, where $f(\varepsilon)$ is the Fermi distribution function, so that

$$\langle\delta g_{\alpha\beta}(\varepsilon)\delta g_{\gamma\delta}(\varepsilon')\rangle = \delta_{\alpha\beta}\delta_{\gamma\delta}G_\nu^2(T) + (\delta_{\alpha\gamma}\delta_{\beta\delta}+\delta_{\alpha\delta}\delta_{\beta\gamma})G_D^2(T), \tag{2.6}$$

$$G_\nu^2(T) = \frac{4}{\beta}\left(\frac{e^2E_{Th}}{\pi}\right)^2\int\frac{d\omega}{2T}F(\omega/2T)\sum_q \mathrm{Re}\left(\frac{1}{Dq^2-i\omega}\right)^2, \tag{2.7}$$

$$G_D^2(T) = \frac{4}{\beta}\left(\frac{e^2E_{Th}}{\pi}\right)^2\int\frac{d\omega}{2T}F(\omega/2T)\sum_q \frac{1}{(Dq^2)^2+\omega^2}, \tag{2.8}$$

$$F(z) = \frac{z\coth(z)-1}{\sinh^2(z)}. \tag{2.9}$$

The sensitivity of conductance fluctuations to a variation of the Fermi energy shows up in the temperature dependence of the correlations. At low temperatures $T \ll E_{Th}$, it is sufficient to take $\omega \to 0$ limit in the q-summations of $G^2_{\nu(D)}$ functions since $F(\omega/2T)$ is sharply peaked at zero frequency. In this case both contributions become equal. As an example, suppose that the sample is connected to leads along the x-direction and isolated in the other directions. The leads play the role of a reservoir, and the boundary conditions in that direction correspond to an absorbing wall. The diffusion modes in this direction are thus quantized as $q_x = n_x\pi/L$ with $n_x = 1, 2, \ldots$. In the other directions, the boundary conditions are those of hard walls which implies the same quantization of diffusion modes with the contribution of the mode $n_{y,z} = 0$ added. This results in the q-summation in above expression in the form $\sum_{n_x \neq 0, n_y, n_z}(n_x^2 + n_y^2 + n_z^2)^{-2}$. As a result, in the zero temperature limit (restoring Planck's constant $\hbar$)

$$\langle \delta g_{\alpha\beta}(\varepsilon)\delta g_{\gamma\delta}(\varepsilon')\rangle = \frac{4b_d}{\beta\pi^6}\left(\frac{e^2}{\hbar}\right)^2 (\delta_{\alpha\beta}\delta_{\gamma\delta} + \delta_{\alpha\gamma}\delta_{\beta\delta} + \delta_{\alpha\delta}\delta_{\beta\gamma}), \tag{2.10}$$

with $b_1 = \pi^4/90$, $b_2 \approx 1.51$, and $b_3 \approx 2.52$. This formula shows that conductance fluctuations do not depend on the strength of disorder since the diffusion constant dropped out from the final expression: the fluctuations are said to be universal. They depend only on the sample geometry and time-reversal symmetry. At high temperatures $T \gg E_{Th}$, one finds an algebraic decay of fluctuations $\propto (E_{Th}/T)^p$ with a power exponent depending on dimensionality of the system. The significant dependence of the conductance fluctuations on space dimensionality is a consequence of the diffusive nature of electronic transport.

2.3 Qualitative considerations

We proceed by discussing how results of the previous section will change in superconducting systems close to transition. It has been emphasized early on [43,46] that quantum interference mesoscopic effects may lead to a formation of superconducting droplets that nucleate prior to transition of the whole system. Above T_c there are also thermally induced superconducting fluctuations [19] that are known to be crucially important in describing transport properties. One thus expects that the combined effect of two fluctuation mechanisms may have interesting implications for the kinetic properties of superconductors. Indeed, the probability amplitude of the fluctuations in the pairing gap Δ is controlled by the competition of Cooper pair condensation energy and entropy, and can be estimated from the Ginzburg-Landau functional. The condensation energy exhibits mesoscopic fluctuations with the amplitude $\propto 1/g$ and the correlation radius of the order of thermal length $\sim L_T = \sqrt{D/T}$. Near T_c the latter coincides with the superconducting coherence length $\xi = \sqrt{D/T_c}$. On the other hand, thermal superconducting fluctuations are susceptible to the Ginzburg-Landau correlation length $\xi_T = \xi\sqrt{T_c/(T-T_c)} \gg L_T$ so that mesoscopic fluctuations are almost local with respect to superconducting fluctuations, and thus should be summed randomly from different blocks of the size ξ. For the sample size $L \gg \xi$, the above consideration leads to an estimate of the mesoscopic fluctuations of the critical temperature $\delta T_c/T_c \propto (1/g)(\xi/L)^{(4-d)/2}$, where d is the dimensionality of the system. The response functions in superconductors near T_c are governed by the dynamic pair susceptibility propagator $\mathcal{L}(\omega, q) \propto (Dq^2 + T - T_c + |\omega|)^{-1}$ for a given mode at finite frequency ω and wave vector q, which acquires mesoscopic fluctuations $\delta\mathcal{L} \propto \mathcal{L}^2 \delta T_c$. Even though the whole effect seems to be small, as it scales inversely proportional to conductance, $g \gg 1$, the singular nature of $\mathcal{L}$ at $T - T_c \ll T_c$ as $\{q, \omega\} \to 0$

translates into the substantial temperature dependence of kinetic coefficients. This is the microscopic reason why the universality of mesoscopic effects breaks down in the case of fluctuating superconductors. Following Ref. [58] we elaborate on this point in the context of conductivity fluctuations and then carry out microscopic verification of this result with further extension to thermomagnetic transport.

At the qualitative level the conductivity enhancement near T_c due to superconducting fluctuations can be estimated as

$$\frac{\delta\sigma}{\sigma} \sim \sum_q \langle \Delta_q \Delta_{-q} \rangle \tau_q \sim \frac{1}{g} \left(\frac{T_c}{T - T_c} \right)^{(4-d)/2}, \tag{2.11}$$

where d is dimensionality. In essence this estimate is obtained from the Drude formula for conductivity but applied for fluctuation-induced Cooper pairs. Indeed, the average of pairing gap fluctuations

$$\langle \Delta_q \Delta_{-q} \rangle \simeq \frac{T}{\nu} \frac{1}{Dq^2 + T - T_c} \tag{2.12}$$

measures the average concentration of preformed pairs, while their life-time

$$\tau_q \simeq \frac{1}{Dq^2 + T - T_c} \tag{2.13}$$

at a given mode q is nothing but Ginzburg-Landau relaxation time. Because of its mesoscopic origin, discussed above, fluctuations of T_c lead to a giant mesoscopic fluctuations of the order parameter field $\langle\langle \delta\Delta_q \delta\Delta_{-q} \rangle\rangle$, where double-brackets stand for the thermal and disorder average. Near the critical point

$$\frac{\langle\langle \delta\Delta_q \delta\Delta_{-q} \rangle\rangle}{\langle \Delta_q \Delta_{-q} \rangle} \propto \frac{1}{g} \left(\frac{\xi}{L} \right)^{(4-d)/2} \frac{T_c}{Dq^2 + T - T_c}. \tag{2.14}$$

This yields the estimate for mesoscopic fluctuations of conductivity from squaring Eq. 2.11 in the form

$$\frac{\langle\langle\delta\sigma^2\rangle\rangle}{\sigma^2} \sim \frac{1}{g^4}\left(\frac{\xi_T}{L}\right)^{4-d}\left(\frac{T_c}{T-T_c}\right)^{(8-d)/2}. \tag{2.15}$$

Despite the large factor in the denominator, this expression is substantially more singular than Eq. (2.11) in terms of the temperature dependence near T_c. For concreteness, let's concentrate on the two-dimensional case $d = 2$. Recall that perturbative treatment of the fluctuation effect breaks down beyond the Ginzburg region, so that at most we can allow $T - T_c \sim T_c/g$ when correction to conductivity from Eq. (2.11) becomes of the same order as a bare Drude conductivity. Remarkably, at that temperature scale, and assuming samples size of the order of coherence length $L \sim \xi_T$, the amplitude of mesoscopic fluctuations in conductivity, as estimated from Eq. (2.15), exceeds the bare value by a large parameter $\sqrt{g} \gg 1$.

From these considerations one can infer an estimate of expected fluctuations in thermomagnetic response. This can be achieved by the following lines of reasoning. When subject to crossed electric and magnetic fields, the charged carriers acquire a drift velocity $\bar{v}_x = cE_y/H$ in the x direction (H is in z-direction). That would result in the appearance of a transverse current $J_x = en\bar{v}_x$ with respect to E_y. Under open circuit conditions, no current flows, and the drift of carriers is compensated by the spacial variation of the electric potential $\nabla_x\varphi = -E_x = (enc/\sigma)(E_y/H)$. Because of electroneutrality, this generates the gradient of the chemical potential $\nabla_x\mu(n, T) + e\nabla_x\varphi = 0$, which ultimately corresponds to the appearance of the temperature gradient $\nabla_x T = (d\mu/dT)^{-1}\nabla_x\mu$ along the x direction. Hence, the Nernst coefficient $\nu = E_y/H(-\nabla_x T)$ can be expressed in terms of the full temperature derivative of the chemical potential $\nu = (\sigma/e^2nc)(d\mu/dT)$. This result can be checked for a

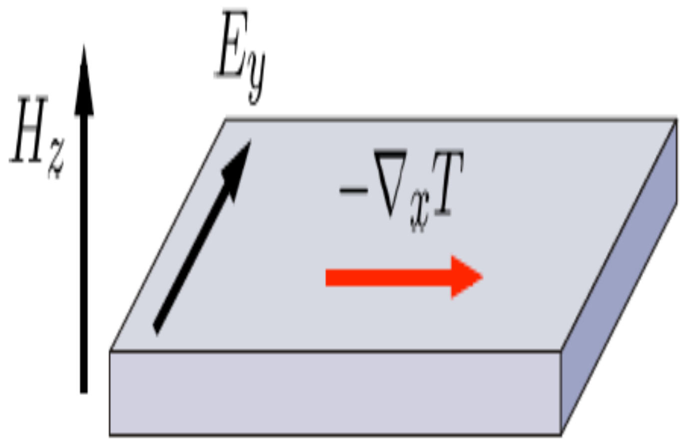

Figure 2.1: The layout of the Nernst experiment: by applying a temperature gradient ($-\nabla T$) in the presence of magnetic field, an electric field is generated.

degenerate electron gas; the chemical potential $\mu(T) = \mu_0 - (\pi^2 T^2/6)(d \ln \nu/d\mu)$ reproduces the Sondheimer formula $\nu = (\pi^2 T/3mc)(d\tau/d\mu)$, where τ is the elastic scattering time. For the preformed Cooper pairs, $d\mu/dT = -1$ so that $\nu \propto \sigma$ and fluctuations in ν should follow that of conductivity. This conjecture will be verified with a microscopic calculation in Sec 2.6.

2.4 Definitions and assumptions

We start with the definition of kinetic coefficients concentrating on the linear response analysis. The electric $\mathbf{J}^e_{tr}$ and heat $\mathbf{J}^h_{tr}$ transport currents are related to the electric field $\mathbf{E}$ and temperature gradient ∇T by the following matrix

$$\begin{pmatrix} \mathbf{J}^e_{tr} \\ \mathbf{J}^h_{tr} \end{pmatrix} = \begin{pmatrix} \sigma & \alpha \\ \overline{\alpha} & \kappa \end{pmatrix} \begin{pmatrix} \mathbf{E} \\ -\nabla T \end{pmatrix}, \tag{2.16}$$

where σ is the electric conductivity tensor , α and $\overline{\alpha}$ are the thermoelectric tensors ($\overline{\alpha} = T\alpha$ due to Onsager relations), and κ is the thermal conductivity tensor. Applying the open circuit conditions to Eq. (2.16) (see Figure 2.1 for the layout of the experiment), we have $E/\nabla T = \sigma^{-1}/\alpha$ where the inverse of σ is

$$\sigma^{-1} = \frac{1}{\det|\sigma|} \begin{pmatrix} \sigma_{yy} & -\sigma_{xy} \\ -\sigma_{yx} & \sigma_{xx} \end{pmatrix}.$$

Multiplying it by α, taking the corresponding element of the matrix, the Nernst coefficient is expressed in terms of the conductivity and thermoelectric tensors

$$\nu = \frac{E_y}{(-\nabla_x T)H} = \frac{1}{H}\frac{\alpha_{xy}\sigma_{xx} - \alpha_{xx}\sigma_{xy}}{\sigma_{xx}^2 + \sigma_{xy}^2}. \tag{2.17}$$

An important aspect of the calculation of the transverse thermoelectric response α_{xy}, discussed in detail in Ref. [84], is the need to account for bulk magnetization currents. This issue arises because the microscopic electric and heat currents, as calculated below by the Kubo formula, are composed of transport and magnetization currents

$$\mathbf{J}^e = \mathbf{J}^e_{tr} + \mathbf{J}^e_{mag}, \quad \mathbf{J}^h = \mathbf{J}^h_{tr} + \mathbf{J}^h_{mag}. \tag{2.18}$$

The magnetization currents are currents that circulate in the sample and do not contribute to the net currents which are measured in a transport experiment. On the other hand, they do contribute to the total microscopic currents, and it is thus necessary to subtract them from the total currents to obtain the transport current response. In the presence of an applied electric field, it was shown in Ref. [84] that the magnetization current is given by

$$\mathbf{J}^h_{mag} = c\mathbf{M} \times \mathbf{E}, \tag{2.19}$$

where $\mathbf{M}$ is the equilibrium magnetization (in the absence of the electric field). It then follows that the transverse thermoelectric response is given by

$$\alpha_{xy} = -\frac{J^h}{E_x T} + \frac{cM_z}{T} = \bar{\alpha}_{xy} + \frac{cM_z}{T}. \tag{2.20}$$

It is apparent from the above expression that α_{xy} is obtained by subtracting the result of two independent calculations: the response of the total current to the applied electric and magnetic fields, and the magnetization currents as derived from the equilibrium magnetization. Therefore, we need to know magnetic susceptibility $\mathbf{M} = \chi\mathbf{H}$, which will be computed diagrammatically along with $\bar{\alpha}_{xy}$. Importance of the magnetization contribution to α_{xy} in the context of superconducting fluctuations was elaborated by Ussishkin [74].

The calculations will be carried out assuming particle-hole symmetry, i.e., neglecting any contributions which arise due to asymmetry around the Fermi surface in properties such as the density of states or scattering time. Particle-hole symmetry implies that $\sigma_{xy} = \alpha_{xx} = \kappa_{xy} = 0$, and therefore the general expression for the Nernst coefficient Eq. (2.17) greatly simplifies. The conventional result for α_{xy} in the normal metallic state (so-called quasiparticle contribution) also vanishes in this limit. However, it has been emphasized [74] that this result is not required by the symmetry, and will not necessarily hold when additional processes, such as superconducting or mesoscopic fluctuations, are taken into account without breaking the particle-hole symmetry. Another simplification of our analysis comes from assuming s-wave

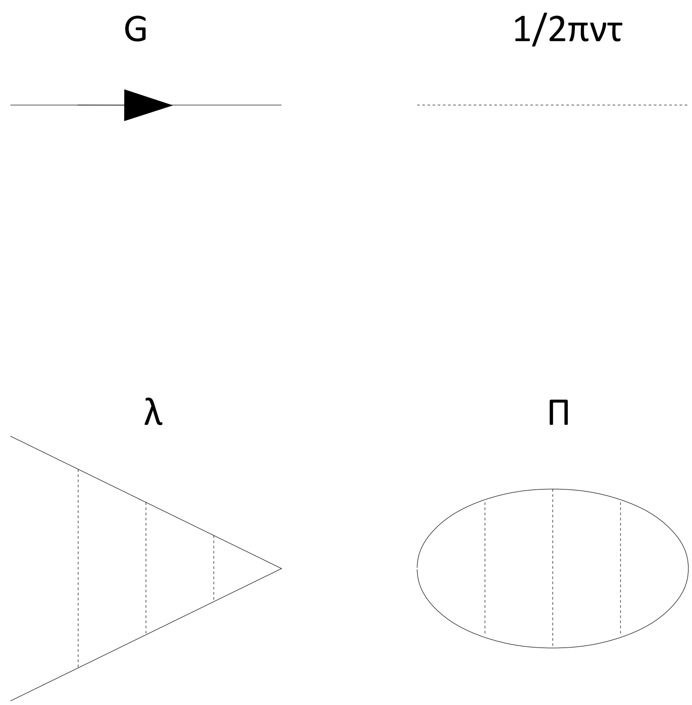

Figure 2.2: Building blocks of the diagrammatic technique. Straight lines represent disorder-averaged single-particle Green's functions. The straight-dashed lines represent single impurity lines that carry an overall factor $1/2\pi\nu_d\tau$ in the diagrams. The vertex function $\lambda(\varepsilon, \varepsilon', q)$ is drawn in the ladder approximation, while diagrams with the crossed impurity lines yield parametrically smaller contributions in $1/g \ll 1$. The polarization operator $\Pi(\omega, q)$ ("bubble" diagram) is also presented in the main ladder approximation.

symmetry of the superconducting order parameter. In the context of the high-temperature superconductors, it is of interest to consider also the case of d-wave symmetry in a similar approach.

2.5 Technical prerequisites

In our calculations we closely follow Ref. [19] for all the basic definitions and notations of the diagrammatic technique. Graphical rules for constructing Feynman diagrams in the context of transport in the disordered systems are depicted in Fig. 2.2. We start from the disorder averaged single particle Green's function, which in the energy and momentum (ε, p) representation reads

$$\mathcal{G}(\varepsilon, p) = \frac{1}{\varepsilon - \xi_p + \frac{i}{2\tau}\mathrm{sgn}\varepsilon}, \quad \xi_p = p^2/2m - \varepsilon_F, \tag{2.21}$$

where τ is the elastic scattering time on impurities. In the parameter $T\tau$ one should distinguish three different transport regimes in fluctuating superconductors: the diffusive scattering $T\tau \ll 1$, the ballistic limit $1 \ll T\tau \ll \sqrt{T_c/(T-T_c)}$, and the ultra-clean limit $T\tau \gg \sqrt{T_c/(T-T_c)}$. We will concentrate on the diffusive case exclusively, which is also mathematically simpler. In the ballistic case, fluctuation effects become strongly non-local in space, while diffusive impurity scattering makes response functions isotropic and local.

The basic building block of the Cooper ladder is two Green's functions connected by one impurity line, which we denote by Γ. Each impurity line brings a factor $1/2\pi\nu_d\tau$, where ν_d is the density of states. In two-dimensional case $\nu_2 = m/2\pi$, so that

$$\Gamma(\omega, q) = \frac{1}{2\pi\nu_d\tau}\int\frac{d^dp}{(2\pi)^d}\mathcal{G}^R(\varepsilon_+, p_+)\mathcal{G}^A(\varepsilon_-, p_-), \tag{2.22}$$

where superscript $R(A)$ stands for the retarded (advanced) component of Eq. (2.21). We used shorthand notations $\varepsilon_\pm = \varepsilon \pm \omega/2$ and $p_\pm = p \pm q/2$. Integrating above over ξ_p and expanding to the first order in $\omega\tau, Dq^2\tau \ll 1$,

$$\Gamma(\omega, q) = 1 + \tau(i\omega - Dq^2), \tag{2.23}$$

where $D = v_F^2\tau/2$ is the diffusion coefficient (here and in the remaining parts of the thesis we concentrate of the two-dimensional case unless otherwise explicitly mentioned). Having

Γ one can sum up the whole series of ladder diagrams to obtain the Cooperon propagator

$$\mathcal{C}(\omega, q) = \frac{1}{2\pi\nu_d\tau}(1 + \Gamma + \Gamma^2 + \ldots) = \frac{1}{2\pi\nu_d\tau}\frac{1}{1-\Gamma} = \frac{1}{2\pi\nu_d\tau^2}\frac{1}{Dq^2 - i\omega}. \tag{2.24}$$

In practice it is also useful to have the same expression but rewritten in the Matsubara representation with two different energies $\varepsilon_{1,2}$ running through each of the Green's function lines of the Copper ladder

$$\mathcal{C}(\varepsilon_1, \varepsilon_2, q) = \frac{1}{2\pi\nu_d\tau^2}\frac{\theta(-\varepsilon_1\varepsilon_2)}{Dq^2 + |\varepsilon_1 - \varepsilon_2|}, \tag{2.25}$$

where $\theta(x)$ is the unity step-function. The vertex function dressed with impurities is represented as follows (see Fig. 2.2)

$$\lambda(\varepsilon_1, \varepsilon_2, q) = 2\pi\nu_d\tau\mathcal{C}(\varepsilon_1, \varepsilon_2, q). \tag{2.26}$$

The propagator of superconducting fluctuations reads

$$\mathcal{L}^{-1}(\omega, q) = -\lambda_{sc}^{-1} + \Pi(\omega, q), \tag{2.27}$$

where λ_{sc} is the coupling constant in the particle-particle (Cooper) channel and

$$\Pi(\omega, q) = 4\pi\nu_d T\sum_{\varepsilon_n > 0}\frac{1}{2\varepsilon_n + |\omega| + Dq^2} \tag{2.28}$$

is the polarization operator (summation goes over the fermionic Matsubara frequency $\varepsilon_n = (2n+1)\pi T$, while $\omega_m = 2\pi mT$ corresponds to bosonic frequency). With these ingredients

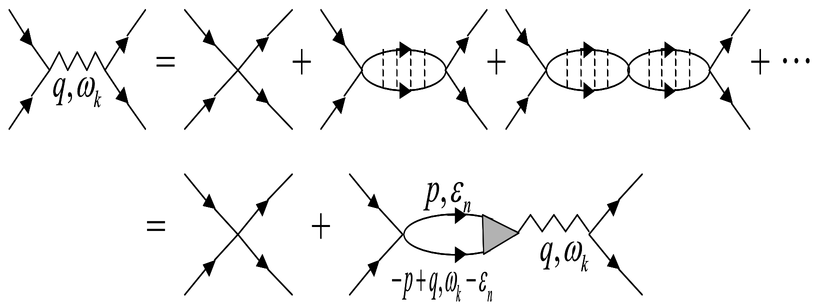

Figure 2.3: The Dyson equation for the fluctuating propagator $\mathcal{L}(\omega, q)$ which represented graphically as the wavy line and computed in the ladder approximation. Solid lines represent one-electron Green's function, greay triangle is the impurity dressed effective vertex, while each cross between two Green's functions is associated with the electron-electron coupling constant $-\lambda_{sc}$.

at hand one can explicitly calculate the pair propagator which takes the form (see Fig. 2.3)

$$\mathcal{L}^{-1}(\omega, q) = -\nu_d \left[\ln \frac{T}{T_c} + \psi\left(\frac{1}{2} + \frac{Dq^2 + |\omega|}{4\pi T}\right) - \psi\left(\frac{1}{2}\right)\right], \tag{2.29}$$

where $\psi(x)$ is the digamma function, and the critical temperature is expressed through the coupling constant $T_c = (2\gamma_E \omega_D/\pi)e^{-1/\nu_d \lambda_{sc}}$ with $\gamma_E = 1.78$ being the Euler constant and ω_D being the Debye frequency, which cuts logarithmically divergent summation at $n_{max} = \omega_D/2\pi T$ in the polarization operator. At small frequencies and momenta (the most relevant limit for most of the further applications) one can expand digamma functions at small argument $\{Dq^2, \omega\}/T \ll 1$ and use $\psi'(1/2) = \pi^2/2$ to obtain a simpler expression

$$\mathcal{L}(\omega, q) = -\frac{1}{\nu_d} \frac{1}{\ln(T/T_c) + \pi Dq^2/8T + \pi|\omega|/8T}. \tag{2.30}$$

For the purpose of calculating kinetic coefficients, the crucial objects are current vertices. In particular, the electric current vertex function consists of three Green's functions with two impurity ladders

$$
\begin{aligned}
\mathcal{B}^e_i(\omega_m,\Omega_k,q) = 2eT\sum_{\varepsilon_n}\lambda(\varepsilon_n+\Omega_k,\omega_m-\varepsilon_n,q)\lambda(\varepsilon_n,\omega_m-\varepsilon_n,q) \\
\times\sum_p v_i(p)\mathcal{G}(\varepsilon_n+\Omega_k,p)\mathcal{G}(\varepsilon_n,q)\mathcal{G}(\omega_m-\varepsilon_n,q-p),
\end{aligned}
\tag{2.31}
$$

where Ω_k is the external frequency (which will be eventually set to zero in the Kubo formula to get dc-transport coefficient). Being a function of three frequencies and momentum, this vertex is fairly complicated, however in the classical region of fluctuations near T_c its evaluation is straightforward. The essential simplification comes from the separation of energy scales. Bosonic modes are pinned to the energy set by the pole structure of superconducting propagator $Dq^2 \sim |\omega_m| \sim T - T_c$, which can be readily seen from Eq. (2.30). At the same time all fermionic modes are governed by the temperature $|\varepsilon_n| \sim T$. Near the transition $T - T_c \ll T$ we can evaluate the vertex function by setting all the bosonic frequencies to zero. As stated above, within the linear response Kubo analysis the external frequency is also set to zero. As a result, we approximate

$$
\mathcal{B}^e_i(0,0,q) = 2eT\sum_{\varepsilon_n}\lambda^2(\varepsilon_n,-\varepsilon_n,q)\sum_p v_i(p)\mathcal{G}^2(\varepsilon_n,p)\mathcal{G}(-\varepsilon_n,q-p). \tag{2.32}
$$

Transforming now momentum summation into the integral $\sum_p\ldots\to\nu_d\int d\xi_p\langle\ldots\rangle_\vartheta$, where averaging goes along the Fermi surface, and using Eq. (2.21) we get

$$
\mathcal{B}^e_i(0,0,q) = -2e\nu_dT\sum_{\varepsilon_n}\lambda^2(q,\varepsilon_n,-\varepsilon_n)\int_{-\infty}^{+\infty}\frac{d\xi_p}{(i\bar{\varepsilon}_n-\xi_p)^2}\left\langle\frac{v_i(p)}{i\bar{\varepsilon}_n+\xi_p-v_j(p)q_j}\right\rangle_\vartheta, \tag{2.33}
$$

where in addition we used $\xi_{q-p}\approx\xi_p-\mathbf{v}\cdot\mathbf{q}$ and abbreviated $\bar{\varepsilon}_n=\varepsilon_n+1/2\tau$. From here we need only the leading small-q part of the vertex. Expanding the denominator to the linear order in q and using Eq. (2.26), the above equation transforms into

$$\mathcal{B}_i^e(0,0,q) = -2e\nu_d T\langle v_i v_j q_j\rangle_\vartheta \sum_{\varepsilon_n} \frac{|2\bar{\varepsilon}_n|^2}{|\varepsilon_n|^2} \int_{-\infty}^{+\infty} \frac{d\xi}{(\xi^2+\bar{\varepsilon}_n^2)^2}. \tag{2.34}$$

The remaining ξ-integration, followed by a ε_n-summation, can be completed in the closed form in terms of the digamma function

$$\mathcal{B}_i^e = 2eB_i(q), \qquad \mathcal{B}_i(q) = \nu_d D\tau q_i \left[\psi\left(\frac{1}{2}+\frac{1}{4\pi T\tau}\right) - \psi\left(\frac{1}{2}\right) - \frac{1}{4\pi T\tau}\psi'\left(\frac{1}{2}\right)\right]. \tag{2.35}$$

Focusing on the diffusive case only $T\tau \ll 1$, the above expression simplifies even further

$$\mathcal{B}_i(q) = -2\nu\eta q_i\,, \qquad \eta = \pi D/8T\,. \tag{2.36}$$

We will also need the heat current vertex function

$$\mathcal{B}_i^h(\omega_m,\Omega_k,q) = T\sum_{\varepsilon_n} \frac{i(2\varepsilon_n+\Omega_k)}{2}\lambda(\varepsilon_n+\Omega_k,\omega_m-\varepsilon_n,q)\lambda(\varepsilon_n,\omega_m-\varepsilon_n,q)$$
$$\times\sum_p v_i(p)\mathcal{G}(\varepsilon_n+\Omega_k,p)\mathcal{G}(\varepsilon_n,p)\mathcal{G}(\omega_m-\varepsilon_n,q-p). \tag{2.37}$$

Under the same approximations as specified above one finds

$$\mathcal{B}_i^h = 2i\nu\omega_m\eta q_i = -i\omega_m\mathcal{B}_i(q)\,. \tag{2.38}$$

It should be stressed that such simple expressions for the electrical and heat current vertices are only possible to obtain near T_c. We will see later in the text that in the quantum low temperature regime the above calculation has to be revisited, and frequency dependence of

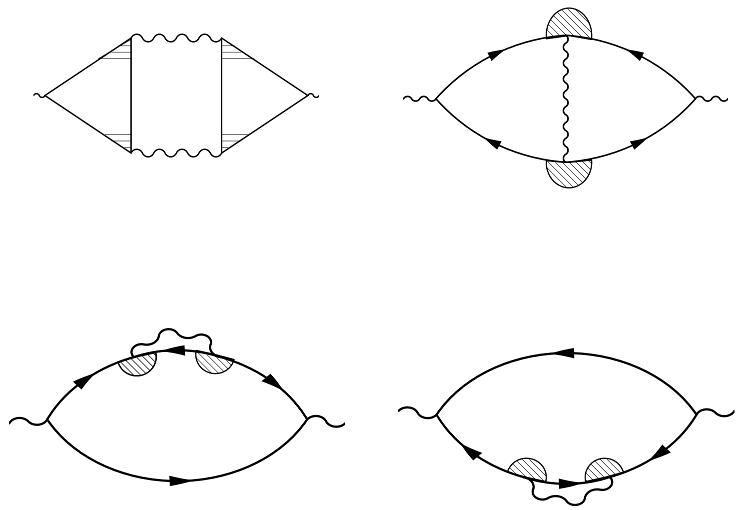

Figure 2.4: Feynman diagrams for the main fluctuation-induced corrections to the conductivity. In the first row we show the Aslamazov-Larkin diagrams (left) and the Maki-Thompson interference diagram (right). In the second row we show two density of states diagrams.

both $\mathcal{B}^e$ and $\mathcal{B}^h$ (omitted here) will play a crucially important role. The above results however are sufficient to make further progress in addressing the classical region of superconducting fluctuations.

As has been discussed in the introductory chapter, the superconducting fluctuations enhance the conductivity above T_c due to so called Aslamazov-Larkin [10] and Maki-Thompson [11,12] contributions as well as density of states effects [18], which are less important for the conductivity unless one studies granular systems. A similar identification of the microscopic contributions applies to other transport coefficients. In the case of the transverse thermomagnetic response, the leading order contribution to α_{xy} is due to the Aslamazov-Larkin (AL) diagrams alone. The contributions of the Maki-Thompson (MT) and density of states (DOS) diagrams are less divergent as $T \to T_c$; see Fig. 2.4 for the identification of diagrams.

Within the linear response analysis, diagonal Aslamazov-Larkin conductivity is determined from the following current-current Kubo kernel K^{ee}_{xx}:

$$\sigma_{xx} = \lim_{\Omega\to 0}\frac{1}{\Omega}\mathrm{Im}[K^{ee}_{xx}(\Omega)]^R\,, \quad K^{ee}_{xx}(\Omega_m) = 4e^2T\sum_{q\omega_k}\mathcal{B}^2_x(q)\mathcal{L}(\omega_k,q)\mathcal{L}(\omega_k+\Omega_m,q)\,, \tag{2.39}$$

where $[K^{ee}_{xx}]^R$ indicates the retarded component of $K^{ee}_{xx}(\Omega_m)$ as it is analytically continued from the discrete Matsubara frequencies into the entire complex plane $i\Omega_m \to \Omega + i0$. The Aslamazov-Larkin contribution to the transversal thermoelectric coefficient is found from the mixed electric current-heat current Kubo response function K^{eh}_{xy}:

$$\bar{\alpha}_{xy} = \frac{H}{cT}\lim_{\Omega,Q\to 0}\frac{1}{\Omega Q}\mathrm{Re}[K^{eh}_{xy}(Q,\Omega_m)]^R, \tag{2.40}$$

where

$$K^{eh}_{xy}(\Omega_m,Q) = -4e^2T\sum_q\mathcal{B}_x(q)\mathcal{B}^2_y(q)\sum_{\omega_n}(i\omega_n + i\Omega_m/2) \tag{2.41}$$
$$\times\left[\mathcal{L}(\omega_n,q-Q_x)\mathcal{L}(\omega_n,q)\mathcal{L}(\omega_n+\Omega_m,q)+\mathcal{L}(\omega_n,q)\mathcal{L}(\omega_n+\Omega_m,q)\mathcal{L}(\omega_n+\Omega_m,q+Q_x)\right]$$

We finally define magnetic susceptibility from the equilibrium magnetization $\mathbf{M} = \chi\mathbf{H}$. Diagrammatically, it may be calculated to linear order in H by considering the current response to a magnetic field at a finite wavevector Q [85]:

$$\chi_{\mu\nu} = -\frac{4e^2}{c^2}\epsilon_{\alpha\gamma\mu}\epsilon_{\beta\kappa\nu}T\sum_{\omega,q}\hat{x}_\gamma\hat{x}_\kappa\mathcal{L}^2(\omega,q)\Pi'_\alpha(\omega,q)\Pi'_\beta(\omega,q), \tag{2.42}$$

where $\epsilon_{\alpha\beta\gamma}$ is the anti-symmetric Levi-Civita unity tensor, and $\hat{x}$ is thecoordinate operator in momentum representation. Below we will consider only the isotropic case $\chi_{\mu\nu} = \chi\delta_{\mu\nu}$. With these ingredients at hand we proceed with the calculation of fluctuation-induced corrections to σ_{xx}, α_{xy}, and χ, as well as their mesoscopic correlation functions $\langle\delta\sigma_{xx}^2\rangle$, $\langle\delta\alpha_{xy}^2\rangle$, and $\langle\delta\chi^2\rangle$ along with the possible cross-correlators.

2.6 Mesoscopic Nernst effect

The first step in the derivation of desired kinetic coefficients within the Kubo formalism requires consideration of the discrete sums over Matsubara frequencies, such as sums in the response kernels of Eqs. (2.39) and (2.41). Such summations over bosonic frequencies can be conveniently done with the help of closed contour integration in the complex plane by using the following formula

$$T\sum_{\omega_m} f(\omega_m) = \frac{1}{4\pi i}\oint d\omega f(-i\omega)\coth\left(\frac{\omega}{2T}\right). \tag{2.43}$$

Applying this to Eq. (2.39) one finds

$$K^{ee}_{xx}(\Omega_m) = 4e^2\sum_q \mathcal{B}_x^2(q)\frac{1}{4\pi i}\oint d\omega\mathcal{L}(-i\omega,q)\mathcal{L}(-i\omega+\Omega_m,q)\coth\left(\frac{\omega}{2T}\right). \tag{2.44}$$

The propagators under the integral have breaks of analyticity in the complex plane of ω at $\mathrm{Im}(\omega)=0$ and $\mathrm{Im}(\omega)=-\Omega_m$, so that the integration contour has two branch cuts along these lines. We delegate details of this integration, followed by an analytical continuation, to Appendix-A and present here only the result for the conductivity correction

$$\sigma_{xx} = \frac{e^2}{\pi T}\sum_q \mathcal{B}_x^2(q)\int_{-\infty}^{+\infty}\frac{d\omega}{\sinh^2(\omega/2T)}[\mathrm{Im}\mathcal{L}^R(\omega,q)]^2. \tag{2.45}$$

For the further integrations we define the following dimensionless units: $x = \eta q^2$, $y = \pi\omega/8T$, and $\epsilon = \ln(T/T_c) \approx (T - T_c)/T_c$. In these units, the interaction propagator and vertex function become

$$\mathrm{Im}\mathcal{L}^R(x,y) = -\frac{1}{\nu}\frac{y}{(\epsilon+x)^2+y^2}\,, \quad \mathcal{B}_x^2(x) = 4\nu^2\eta x\cos^2\phi\,, \tag{2.46}$$

and integrations transform into

$$\sum_q \to \int_0^{2\pi} d\phi \int_0^{\infty} \frac{dx}{8\pi^2\eta}\,, \quad \int_{-\infty}^{+\infty} \frac{d\omega}{\sinh^2(\omega/2T)} \to \frac{\pi T}{2}\int_{-\infty}^{+\infty}\frac{dy}{y^2}\,, \tag{2.47}$$

where we expanded $\sinh y \approx y$ since major contribution comes from the range of parameters $\{x, y\} \sim \epsilon \ll 1$. Combining these definitions together, rescaling $y \to (\epsilon + x)y$ first and then $x \to \epsilon x$, the latter expression transforms into

$$\sigma_{xx} = \frac{e^2}{4\pi^2\epsilon}\int_0^{2\pi} d\phi\cos^2\phi \int_0^{\infty}\frac{xdx}{(x+1)^3}\int_{-\infty}^{+\infty}\frac{dy}{(1+y^2)^2}\,, \tag{2.48}$$

with the three integrals equal to $\pi, 1/2$, and $\pi/2$, respectively, and thus with the final result

$$\sigma_{xx} = \frac{e^2}{16}\frac{T_c}{T - T_c}. \tag{2.49}$$

So far we have only reproduced the celebrated result of Aslamazov and Larkin [10]. Our immediate task is to generalize this result for mesoscopic effects associated with fluctuations of pair propagator. For that matter we return to Eq. (2.45), take its variation, square the result, and average it over the realization of disorder potential. We thus find

$$
\begin{aligned}
\langle\delta\sigma_{xx}^2\rangle = \frac{4e^4}{\pi^2 T^2}\sum_{q_1 q_2}\mathcal{B}_x^2(q_1)\mathcal{B}_x^2(q_2)\int_{-\infty}^{+\infty}\frac{d\omega_1 d\omega_2}{\sinh^2(\omega_1/2T)\sinh^2(\omega_2/2T)} \\
\mathrm{Im}\mathcal{L}^R(\omega_1,q_1)\mathrm{Im}\mathcal{L}^R(\omega_2,q_2)\langle\mathrm{Im}\delta\mathcal{L}^R(\omega_1,q_1)\mathrm{Im}\delta\mathcal{L}^R(\omega_2,q_2)\rangle.
\end{aligned}
\tag{2.50}
$$

In order to calculate the irreducible correlation function of the pairing susceptibility, one has to draw two diagrams for $\mathcal{L}$ and connect their diffusive parts by impurity lines. Such construction involves four colliding Diffuson-Cooperon ladders and, on a technical level, requires computation of four- and six-order Hikami boxes [86], see Fig. 2.5 for the illustration. Some of these diagrams have been studied before [43,45–47,58] and we invoke that knowledge for our purposes. In particular we use

$$
\langle\delta\mathcal{L}^{R(A)}(\omega_1,q_1)\delta\mathcal{L}^{R(A)}(\omega_2,q_2)\rangle = \frac{A\nu_d^2}{g^2}\left(\frac{L_T}{L}\right)^2[\mathcal{L}^{R(A)}(\omega_1,q_1)]^2[\mathcal{L}^{R(A)}(\omega_2,q_2)]^2. \tag{2.51}
$$

Precise calculation of the numerical factor $A\sim 1$ is not of principal importance in a view of strong dependence of the whole expression on temperature in the low momentum and frequency limit $(\omega,q)\to 0$, which in a way defines T-dependence of transport coefficients. It is then straightforward to show that

$$
\begin{aligned}
&\langle\mathrm{Im}\delta\mathcal{L}^R(\omega_1,q_1)\mathrm{Im}\delta\mathcal{L}^R(\omega_2,q_2)\rangle = \\
&\frac{4A\nu_d^2}{g^2}\left(\frac{L_T}{L}\right)^2\mathrm{Im}\mathcal{L}^R(\omega_1,q_1)\mathrm{Re}\mathcal{L}^R(\omega_1,q_1)\mathrm{Im}\mathcal{L}^R(\omega_2,q_2)\mathrm{Re}\mathcal{L}^R(\omega_2,q_2).
\end{aligned}
\tag{2.52}
$$

We take this back into the equation for $\langle\delta\sigma_{xx}^2\rangle$, and introduce dimensionless x,y,ϵ variables,

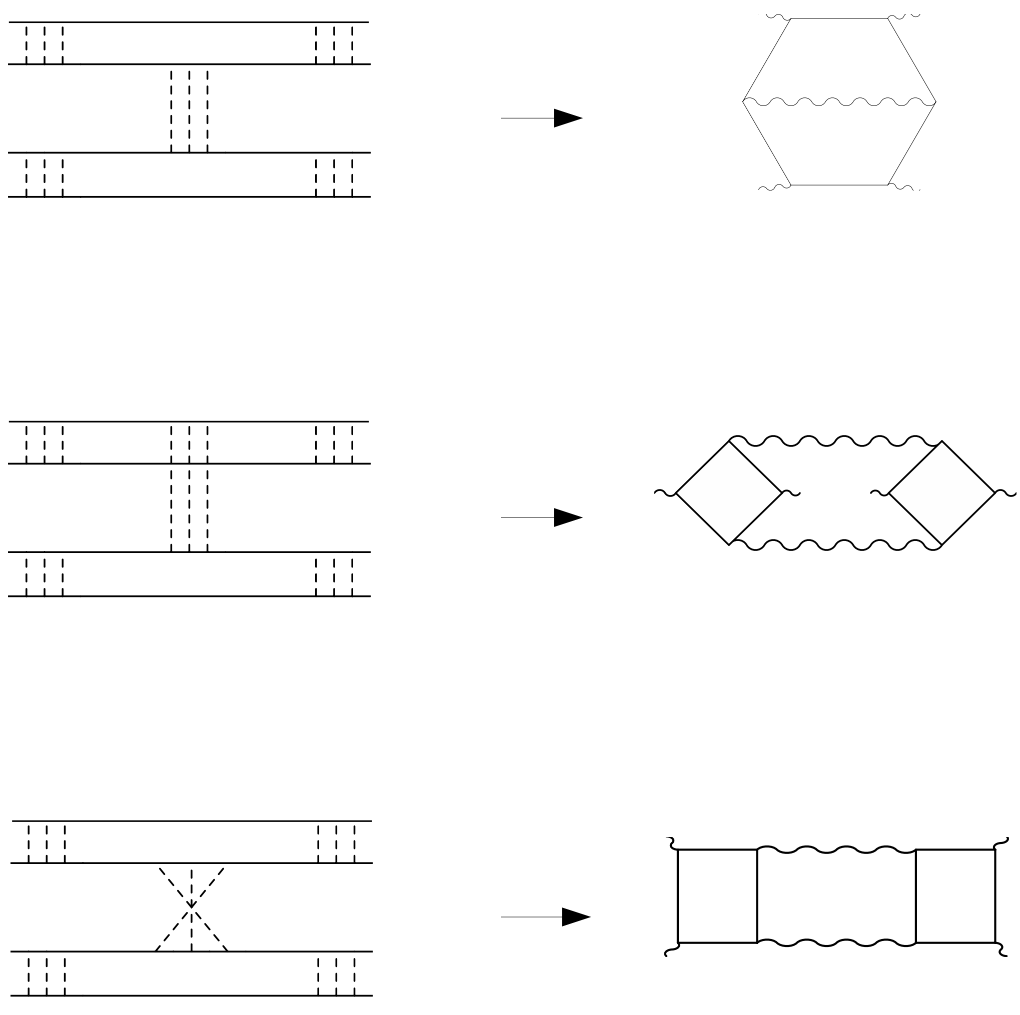

Figure 2.5: Leading order diagrams for the irreducible correlator of mesoscopic disorder-averaged two pair-propagators. This averaging contains collisions of four diffusion or Cooper modes, and involves forth and sixth order Hikami boxes (internal impurity lines are implicit on diagrams).

as in the case considered above, to arrive at

$$\langle\delta\sigma_{xx}^2\rangle = \frac{Ae^4L_T^2}{\pi^4g^2L^2}\int_0^{2\pi}d\phi_1 d\phi_2\cos^2\phi_1\cos^2\phi_2$$
$$\int_0^{\infty}dx_1dx_2\int_{-\infty}^{+\infty}dy_1dy_2\frac{x_1x_2(x_1+\epsilon)(x_2+\epsilon)}{[(x_1+\epsilon)^2+y_1^2]^3[(x_2+\epsilon)^2+y_2^2]^3}, \tag{2.53}$$

that after rescaling of integration variables gives the final result

$$\langle\delta\sigma_{xx}^2\rangle = \frac{Ae^4}{32\pi g^2}\left(\frac{\xi_T}{L}\right)^2\left(\frac{T_c}{T-T_c}\right)^3. \tag{2.54}$$

Thus by microscopic analysis we have confirmed our earlier result Eq. (2.15) which was based on a qualitative considerations. We have already argued that interplay of superconducting and mesoscopic effects trigger giant fluctuations for samples $L \ll \xi_T$ at the temperatures $T - T_c \sim T_c/g$. For larger samples $L \gg \xi_T$, fluctuations saturate to $\langle\delta\sigma_{xx}^2\rangle \sim (e^2/g)^2(T_c/E_{Th})^3$.

We can build on this result to consider emergent mesoscopic fluctuations in the transversal thermoelectric coefficient. We start from Eq. 2.41 where we need only contributions linear in Q, which can be easily extracted by expanding the pair propagator and noticing that

$$\frac{\partial\mathcal{L}(\omega,q)}{\partial q_x} = -\mathcal{B}_x(q)\mathcal{L}^2(\omega,q). \tag{2.55}$$

Next we have to sum the resulting expression for $K_{xy}^{eh}(\Omega_m,Q)$ over the Matsubara frequency, as in the case of the conductivity calculation by contour integration in the complex plane. We find

$$K_{xy}^{eh}(\Omega_m,Q) = -4e^2Q\sum_q\mathcal{B}_x^2(q)\mathcal{B}_y^2(q)\frac{1}{4\pi i}\oint d\omega\coth\left(\frac{\omega}{2T}\right)(\omega+i\Omega_m/2)$$
$$\times[\mathcal{L}^3(\omega,q)\mathcal{L}(\omega+i\Omega_m,q)-\mathcal{L}(\omega,q)\mathcal{L}^3(\omega+i\Omega_m,q)]. \tag{2.56}$$

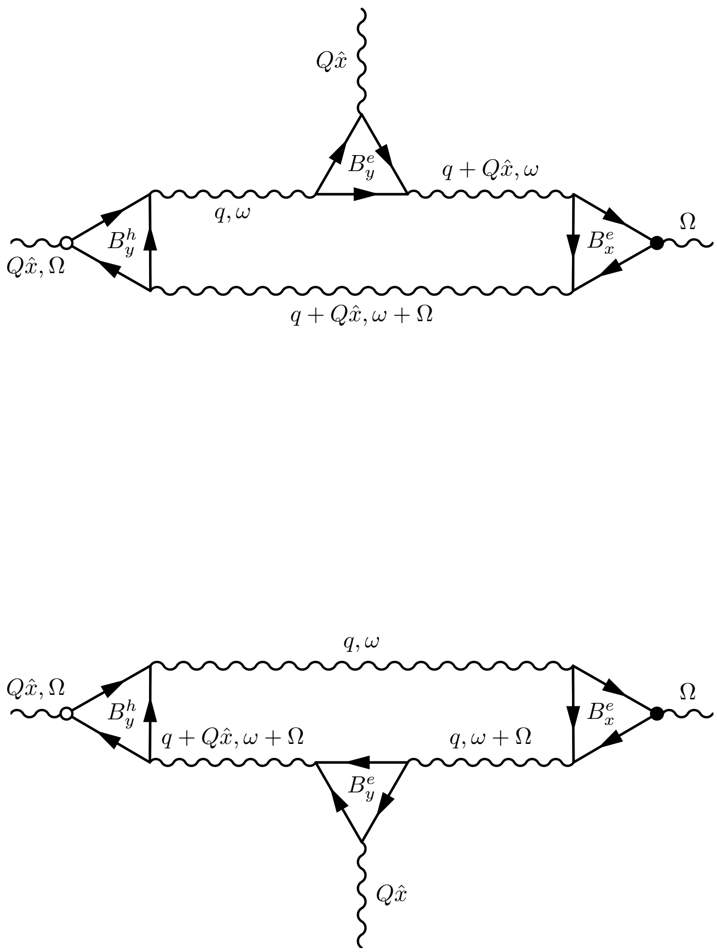

Figure 2.6: The Aslamazov-Larkin diagrams contributing to $K^{eh}_{xy}(\Omega)$. The wavy lines correspond to the fluctuation propagator $\mathcal{L}(q, \omega)$; electric current vertices $\mathcal{B}^e$ and heat current vertices $\mathcal{B}^h$ are indicated in the figure along with running momenta and frequencies.

After further calculation (see analytical continuation that is done carefully in the Appendix-A) we arrive at

$$\bar{\alpha}_{xy} = \frac{4e^2 H}{c\pi T} \sum_q \mathcal{B}_x^2(q)\mathcal{B}_y^2(q) \int_{-\infty}^{+\infty} d\omega \coth\frac{\omega}{2T}$$
$$\times \left\{ [\mathrm{Re}\mathcal{L}^R(\omega,q)]^3 \mathrm{Im}\mathcal{L}^R(\omega,q) + \mathrm{Re}\mathcal{L}^R(\omega,q)[\mathrm{Im}\mathcal{L}^R(\omega,q)]^3 \right\}. \quad (2.57)$$

In the dimensionless units $x = \eta q^2$ and $t = \pi\omega/2T$, and after the rescaling $y \to (x+\epsilon)y$ and $x \to \epsilon x$, one finds at the intermediate step

$$\bar{\alpha}_{xy} = \frac{16 e^2 H}{c\pi^3}\frac{\eta}{\epsilon} \int_0^{2\pi} d\phi \cos^2\phi \sin^2\phi \int_0^{\infty} \frac{x^2 dx}{(x+1)^4} \int_{-\infty}^{+\infty} dy \frac{1}{(1+y^2)^3}. \quad (2.58)$$

After remaining integration, where each of the three integrals yields coefficient $\pi/4, 1/3$, and $3\pi/8$ respectively, one finds

$$\bar{\alpha}_{xy} = \frac{e}{2\pi}\frac{\xi_T^2}{\ell_H^2} \propto \frac{T_c}{T - T_c} \quad (2.59)$$

Here $\ell_H = \sqrt{c/eH}$ is the magnetic length and $\bar{\alpha}_{xy}$ has the same scaling with temperature as the conductivity. As shown by Ussishkin [74] the magnetization contribution has the same structural form but comes with the coefficient $-1/3$ instead of $1/2$ so that $\alpha_{xy} = \bar{\alpha}_{xy} + cM_z/T$ has an overall coefficient of $1/6$.

We can address now the mesoscopic fluctuations of α_{xy} by taking the variation of Eq. (2.57), squaring the result, and averaging over the disorder realization with the help of the correlation function Eq. (2.51). In doing so we encounter quite a cumbersome expression with several contributions to $\langle \delta\alpha_{xy}^2 \rangle$, but we make an observation that all the emergent terms have exactly the same scaling with temperature and differ from each other only by a numerical coefficient of the order of unity. For brevity we present here one particular such term

$$\langle \delta\alpha_{xy}^2 \rangle = A \left(\frac{e^2 \nu_d H L_T}{cgTL} \right)^2 \sum_{q_1 q_2} \mathcal{B}_x^2(q_1)\mathcal{B}_x^2(q_2)\mathcal{B}_y^2(q_1)\mathcal{B}_y^2(q_2) \tag{2.60}$$

$$\int_{-\infty}^{+\infty} d\omega_1 d\omega_2 \coth\frac{\omega_1}{2T} \coth\frac{\omega_2}{2T} [\mathrm{Re}\mathcal{L}^R(\omega_1, q_1)]^4 [\mathrm{Re}\mathcal{L}^R(\omega_2, q_2)]^4 \ \mathrm{Im}\mathcal{L}^R(\omega_1, q_1) \mathrm{Im}\mathcal{L}^R(\omega_2, q_2)$$

and carry out the calculation up to a factor modulo one (we will absorb all the numerical factors into the redefinition of coefficient A). Since most relevant frequencies $\omega \sim T - T_c$ are small compared to temperature we can approximate $\coth(\omega/2T) \approx 2T/\omega$. Transforming the above into dimensionless variables

$$\langle \delta\alpha_{xy}^2 \rangle = \frac{e^2 A}{g^2} \left(\frac{\xi^2 L_T}{\ell_H^2 L} \right)^2 \int_0^{\infty} dx_1 dx_2 \int_{-\infty}^{+\infty} dy_1 dy_2 \frac{x_1^2 x_2^2 (x_1+\epsilon)^4 (x_2+\epsilon)^4}{((x_1+\epsilon)^2 + y_1^2)^5 ((x_2+\epsilon)^2 + y_2^2)^5}, \tag{2.61}$$

followed by rescaling and integration, one finds

$$\langle \delta\alpha_{xy}^2 \rangle = \frac{e^2 A}{g^2} \left(\frac{\xi_T}{\ell_H} \right)^4 \left(\frac{L_T}{L} \right)^2 \left(\frac{T_c}{T - T_c} \right)^2 . \tag{2.62}$$

Interestingly $\langle \delta\alpha_{xy}^2 \rangle$ has exactly the same temperature scaling as $\langle \delta\sigma_{xx}^2 \rangle$, namely $\propto (T - T_c)^{-4}$, that we already anticipated based on qualitative considerations in Sec. 2.3, and the above diagrammatic calculations provide the microscopic justification for our results.

It remains to consider fluctuation-induced corrections to magnetic susceptibility and its mesoscopic fluctuations. From Eq. (2.42) we get for the Aslamazov-Larkin contribution [85]

$$\chi = -\frac{16 e^2}{3c^2} T \sum_{\omega_m, q} \Pi'_x \mathcal{L}^3(\omega_m, q) \left[\Pi'_x \Pi''_{yy} - \Pi'_y \Pi''_{xy} \right], \tag{2.63}$$

where derivatives of the polarization operator can be easily computed from Eq. (2.28)

$$\Pi'_{x,y} = -\frac{\pi\nu D}{4T} q_{x,y}, \qquad \Pi''_{yy} = -\frac{\pi\nu D}{4T}, \qquad \Pi''_{xy} = 0. \tag{2.64}$$

Already at this level, by simple power counting of integration variables, one can deduce that $\chi \propto T_c/(T - T_c)$. Consequently one expects that $\langle\delta\chi^2\rangle$ will also scale with $T - T_c$ in the same way as the conductivity and thermomagnetic coefficients. Indeed,

$$\langle\delta\chi^2\rangle = A\left(\frac{e^2\nu_d^2\eta L_T}{c^2 gL}\right)^2 \sum_{q_1 q_2} \mathcal{B}_x^2(q_1)\mathcal{B}_x^2(q_2) \int d\omega_1 d\omega_2 \coth\frac{\omega_1}{2T}\coth\frac{\omega_2}{2T} \\ \times \mathrm{Im}[\mathcal{L}^R(\omega_1, q_1)]^4 \mathrm{Im}[\mathcal{L}^R(\omega_2, q_2)]^4, \tag{2.65}$$

which, as in the previous examples, reduces with standard steps to

$$\langle\delta\chi^2\rangle = A\left(\frac{e^2 D}{c^2 g}\right)^2 \left(\frac{L_T}{L}\right)^2 \left(\frac{T_c}{T - T_c}.\right)^4 \tag{2.66}$$

Finally, we will not delve into detailed calculation of the possible cross-correlation functions between different kinetic coefficients, and merely state here that all such correlations are of the same order and yield the same temperature dependence.

2.7 Summary

The main results of this Chapter are expressions Eqs. (2.54), (2.62), and (2.66) for variances of different kinetic coefficients in mesoscopic superconductors. Because of the long-range phase coherence developing close to T_c, sample-specific mesoscopic fluctuations should be observable at large length scales. Similarly to normal samples, these fluctuations are sensitive to magnetic field strength, impurity configuration, and gate voltage. However, in sharp contrast to the normal case, where such fluctuations are universal, interaction effects in the Cooper channel trigger a great amplification of fluctuations due to pairing correlations. This interplay of coherent impurity scattering and interactions leads to a spectacular example of quantum mesoscopic phenomena occurring at a macroscopic scale. Despite the fact that mesoscopic fluctuations are no longer universal, in the sense of random matrix theory classification, we have discovered a different kind of universality in the sense of temperature dependence, which was found to be consistently the same for all the considered kinetic coefficients.

These calculations have been carried out for homogeneously disordered superconductors. Therefore, our results cannot be directly compared to the existing experimental findings where the samples were granular in their origin [33–36]. Granularity adds another parameter into the model – inter-grain conductance – which leads to a strong competition between Aslamazov-Larkin, Maki-Thompson, and DOS effects [87]. Nonetheless, the main features predicted by the theory should be present for inhomogeneously disordered superconductors as well. Indeed, the predicted sample-specific conductance fluctuations were observed experimentally in samples of macroscopic length, and only in a narrow temperature range in the immediate vicinity of T_c, consistent with the theory. The amplitude of the conductance fluctuations was found to greatly exceed that of the UCF in normal samples. It should be also emphasized that some other features accompanying giant mesoscopic effects, such as suppression of $h/2e$ oscillations in cylindrical samples, negative mangetoresistance, and its asymmetry, can be also addressed within the same theoretical model. As of today we are unaware of experimental measurements of mesoscopic effects in thermomagnetic transport of superconductors, except for the measurements of magnetic susceptibility [88]. The mesoscopic Nernst effect has been studied experimentally only in the non-superconducting systems [89]. Verification of the temperature scaling and the overall magnitude of the effect for mesoscopic fluctuations of the Nernst coefficient predicted here would provide an important test for our understanding of thermomagnetic transport phenomena in correlated systems.

Chapter 3

Transport anomalies in Pauli-limited superconductors

3.1 History of the subject

According to the microscopic BCS theory [9] a magnetic field H extinguishes superconductivity. In the absence of spin-orbit interaction there are two basic mechanisms. The first one is the diamagnetic effect associated with the action of the field on the orbital motion of electrons forming a Cooper pair. The second, paramagnetic mechanism, is due to Zeeman splitting of the states with the same spatial wave function but opposite spin. In the former case, the estimate for the upper critical field follows from the condition $H_{c2}\xi^2 \simeq \Phi_0$, where $\Phi_0 = hc/2e$ is the flux quantum. In contrast, Zeeman splitting destroys superconductivity at a different critical field H_z that follows from the condition $E_z \simeq \Delta$, where $E_z = g_L\mu_B H$ is the Zeeman energy, $\mu_B = e\hbar/2mc$ is the Bohr magneton and g_L is the renormalized giro factor, while Δ is the superconducting gap. The ratio between the two fields is $H_z/H_{c2} \sim k_F\ell \sim g \gg 1$, where k_F is Fermi momentum and ℓ is the elastic scattering length. Thus, in bulk systems, the

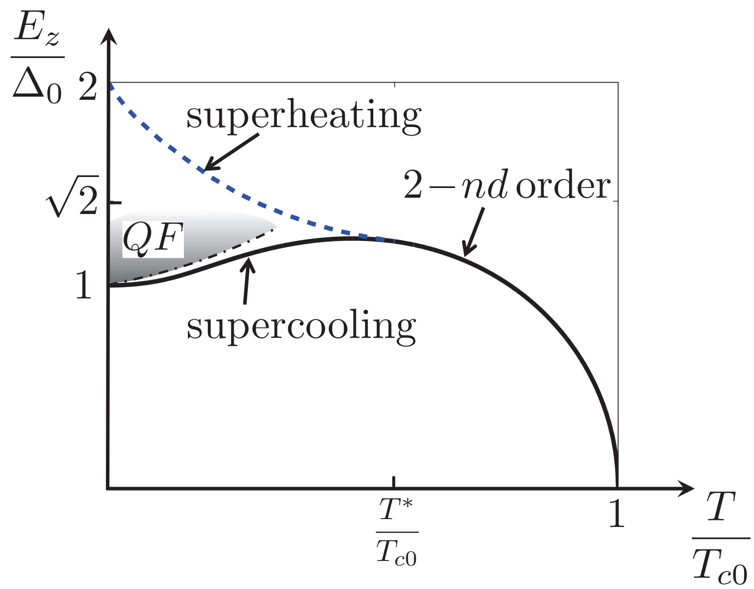

Figure 3.1: Above the tricritical point T^* the second order paramagnet to superconductor transition occurs along the (black) solid line obtained from Eq. 3.1. At $T < T^*$ this line becomes a supercooling part of the hysteresis, and the dashed line is its superheating part. The latter is obtained following Ref. [95]. The grey shaded area with the critical point $(0, \Delta_0)$ as its lowest corner bounded by the black dashed line marks the region of quantum fluctuations (QF).

suppression of superconductivity is typically governed by the first diamagnetic mechanism. The situation changes in the case of restricted dimensionality. For example, in the case of a thin-film superconductor in a parallel field, the above ratio becomes $H_z/H_{c2} \sim (k_F\ell)(d/\xi)$, which can be small provided that the film is thin enough $d \ll \xi/k_F\ell$, such that spin effects dominate.

The scenario of paramagnetically limited superconductivity has a long history that goes back to pioneering works by Clogston and Chandrasekhar [90, 91]. The first order phase transition from superconductor to paramagnet was predicted at the critical field approaching $E_z = \sqrt{2}\Delta$ at low temperatures. In practice, the measured film resistance follows a hysteresis loop [92–96] instead of a sharp first order transition, and the experimental phase diagram is qualitatively as in Fig. 3.1. At low temperatures, the system remains superconducting as the field increases up to the superheating field; above the critical field, the film is trapped in a metastable state. At fields exceeding the superheating threshold the film becomes normal. When the field is reduced, the film stays normal down to the supercooling field $E_z^{sc}(T)$, which corresponds to the zero binding energy of a Cooper pair. At $T = 0$, the normal state is metastable in the interval $\Delta < E_z < \sqrt{2}\Delta$ [97,98]. One should ote that these papers also predicted spatially inhomogeneous state for $\sqrt{2} < E_z/\Delta < 1.52$. We neglect such possibility in this work.

In this Chapter, we study the transport properties near the supercooling field, which is determined by the equation [99]

$$\ln\left(\frac{T_c}{T_{c0}}\right) = \psi\left(\frac{1}{2}\right) - \mathrm{Re}\,\psi\left(\frac{1}{2} + \frac{iE_z^{sc}}{4\pi T_c}\right) \tag{3.1}$$

similar to that in the theory of paramagnetic impurities [100]. Here ψ is the digamma function and $T_{c0} = T_c(H = 0)$ is the critical temperature in the absence of a magnetic field. The zero temperature solution of Eq. 3.1, $E_z^{sc}(0) = \Delta$, defines the quantum critical point (QCP), which is the premier interest of our study. Since in this case the critical parameter depends on H, it allows for a well controlled exploration of the QCP and its vicinity by varying the applied magnetic field.

In the scenario when orbital effects dominate the phase diagram is determined by a similar equation

$$\ln\left(\frac{T_c}{T_{c0}}\right) = \psi\left(\frac{1}{2}\right) - \psi\left(\frac{1}{2} + \frac{\alpha}{4\pi T_c}\right) \tag{3.2}$$

where pair-breaking parameter $\alpha \sim \tau_d^{-1}$ can be deduced from the time-scale of the loss of phase coherence of the Cooper pairs in the presence of the finite magnetic field $\tau_d^{-1} \sim DH^2d^2/\Phi_0^2$. This transition is of the second order throughout the entire $H - T$ line, see

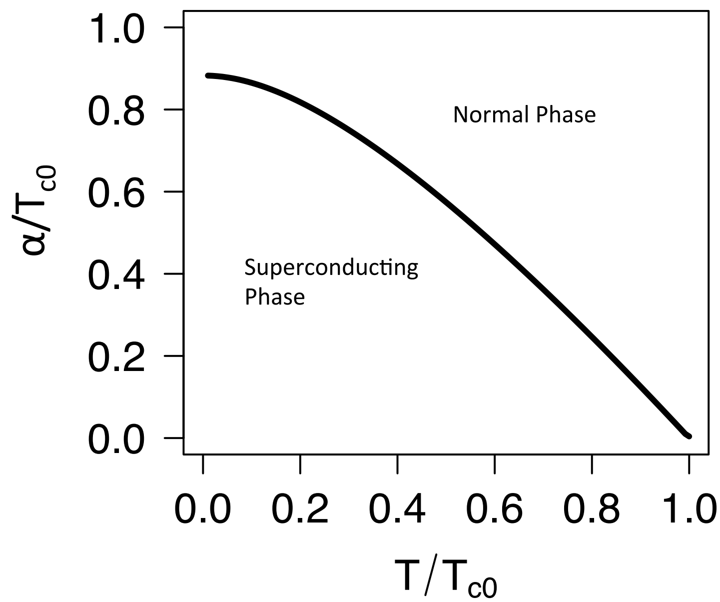

Figure 3.2: Phase diagram of a superconducting thin film in a parallel magnetic field parametrized by pair breaking parameter $\alpha = D(eHd)^2/6$ due to orbital mechanism. $T_{c0} = T_c(H = 0)$ is the critical temperature in the absence of a magnetic field. At $T = 0$ the superconductivity breaks down at the critical value $\alpha_c = \pi T_{c0}/2\gamma_E$, where $\ln \gamma_E \approx 0.577$ is the Euler constant.

Fig. 3.2. Despite apparent similarity between the two cases at the level of the phase diagram, we will demonstrate that the microscopic nature of the fluctuation-induced transport near respective QCPs is conceptually different.

Equation (3.2) implicitly defines the critical temperature T_c as a function of the pair-breaking parameter α. A full analytic solution of this equation in terms of $T_c(\alpha)$ is not possible, but asymptotic expressions can be easily extracted. For $\alpha \ll T_{c0}$ we can expand the digamma function $\psi(x + 1/2)$ to first order in x and thus obtain

$$\ln\left(\frac{T_{c0}}{T_c(\alpha)}\right) - \frac{\pi^2}{2}\frac{\alpha}{4\pi T_c(\alpha)} = 0. \tag{3.3}$$

To first order in α this yields $T_c(\alpha) \approx T_{c0} - \pi\alpha/8$. The expansion for large values of α is a bit more involved, because there exists a critical value of the pair-breaking parameter α_c at which the critical temperature vanishes nonanalytically as a function of α. In order to see this, we rewrite (3.2) in the following form

$$\frac{T_{c0}}{T_c(\alpha)} = \exp\left[\psi\left(\frac{1}{2} + \frac{\alpha}{4\pi T_c(\alpha)}\right)\right] \exp\left[-\psi\left(\frac{1}{2}\right)\right]. \tag{3.4}$$

Since we are in the regime where α is finite but T_c goes to zero, we make use of the asymptotic expansion $\exp[\psi(x+1/2)] \approx x + 1/(4!x) + \dots$ being valid for large x. This expansion yields

$$\frac{T_{c0}}{T_c} \approx 4\gamma_E \left(\frac{\alpha}{4\pi T_c} + \frac{1}{4!(\alpha/4\pi T_c)}\right). \tag{3.5}$$

The critical pair-breaking parameter is defined as the value at which the critical temperature vanishes $T_c(\alpha_c) = 0$. In this case we can neglect the second term on the right hand side of the above equation and obtain $\alpha_c = \pi T_{c0}/2\gamma_E \approx 0.88 T_{c0}$. Expressed in terms of this quantity the critical temperature becomes $T_c \approx (\sqrt{6}/\pi)\sqrt{\alpha(\alpha_c - \alpha)}$.

3.2 Motivation and qualitative picture

The renewed interest in the physics of paramagnetically limited superconductors is motivated by the rapid growth of its experimental realizations. Recent parallel magnetic field studies of two-dimensional superconducting systems were extended to much lower temperatures thus making it feasible to approach the limit of QCP. Tunneling spectroscopy of ultrathin Al and Be films revealed field-induced spin mixing and anomalous resonances in the density of states (DOS) [94, 101, 102]. The latter was successfully explained in theory [103–105], which emphasized the crucial role of superconducting pairing correlations in the paramagnetic state even far from the transition region. A surprising enhancement of superconductivity by a parallel magnetic field, deduced from the transport measurements, was observed in ultrathin, homogeneously disordered amorphous Pb films and in the two-dimensional electron gas realized at the interface of oxide insulators $LaAlO_3$ and $SrTiO_3$ [106]. In addition, pronounced negative magnetoresistance (NMR), concomitant with the enhanced T_c, was reported. Although we do not dwell onto the issue of T_c enhancement in these systems (see Ref. [107] for the recent theoretical proposals), we show that transport anomalies, such as NMR, can be successfully addressed within BCS theory.

The issue of NMR in superconductors, either near the QCP or near the parallel field-tuned superconductor-insulator transition, was previously discussed in the literature experimentally [108, 109] and attributed theoretically [110–112] to the proliferation of superconductive fluctuations. These studies emphasized mainly the orbital effect of a magnetic field on the preformed Cooper pairs. In this Chapter we develop transport theory of paramagnetically limited ultrathin superconductors focusing on the quantum regime of zero temperature near the critical Zeeman field. The regime of classical fluctuations was partially discussed in the early papers [113–116].

The conceptual difference of our analysis from the problem of fluctuation-induced transport close to T_c is that unpaired particles, have finite excitation energy E_z. As a result, the activation probability of such pairs is suppressed exponentially $\propto \exp(-E_z/T)$ at low temperature with the statistical Boltzmann factor. We argue that, while in the standard case the real gapless pairs are only important in the paramagnetically limited case, such pairs are always *virtual*.

Let us illustrate this point by taking the Aslamazov-Larkin correction to the conductivity as an example. Consider first the standard case of near–T_c. In the AL diagram the triangular vertex can be estimated as $\mathcal{B}(\omega, \Omega, q) \propto Dq_x \partial \Pi(\omega, q)/\partial\omega$. At small momenta we can take $\Pi(\omega, 0)$ in a clean system. The imaginary part of the polarization operator $\mathrm{Im}\Pi \approx \int d\xi [n(-\xi_p + \omega)n(\xi_p) - \tilde{f}(-\xi_p + \omega)\tilde{f}(\xi_p)]\delta(\omega - 2\xi) = \nu(\omega/2)\tanh(\omega/2T)$, where the particle and hole occupation numbers are $f(\varepsilon) = (1 + e^{\varepsilon/T})^{-1}$, $\tilde{f}(\varepsilon) = 1 - f(\varepsilon)$. The real part, due to virtual pairs $\mathrm{Re}\Pi(\omega, q) \approx \ln|(\omega^2 - T^2)/\omega_D^2|$, is the familiar Cooper logarithm. The imaginary part contribution $\mathcal{B}(\omega, \Omega, q) \propto Dq_x/T$. In contrast, the real part contribution vanishes at $\omega = 0$ due to the particle-hole symmetry, $\nu(\omega) = \nu$. The expansion in $\omega \sim T - T_c \ll T$ yields a correction small in the parameter $(T - T_c)/T_c \ll 1$.

In the presence of a Zeeman field the situation is very different. The pair activation rate, $\mathrm{Im}\Pi(\omega, q) \approx \nu(\omega)[f(\omega/2 - E_z/2) - f(\omega/2 + E_z/2)]$, gives an exponentially suppressed contribution $\propto Dq_x \exp(-E_z/T)/T$. The real part, due to virtual pair excitation, can be obtained by the Kramers-Kronig relation, $\mathrm{Re}(\omega, q)\Pi \approx \ln|(\omega^2 - E_z^2)/\omega_D^2|$. Its contribution to $\mathcal{B}(\omega, \Omega, q)$ is suppressed only algebraically $\propto Dq_x T/E_z^2$. Unlike the standard case the virtual quasiparticles make a dominant contribution to the triangular vertex excitations. The algebraic suppression of vertexes is most pronounced in the case of the AL and is manifested in additional factors of Dq^2 and ω in σ^{AL}, which makes it logarithmic in $E_z/(E_z - \Delta_0)$. Note that in the case of the near–H_{c2} problem [110] the AL contribution is also suppressed due to the current matrix elements connecting adjacent Landau levels. The regular MT and DOS contributions are proportional to a second derivative of the real part of the polarization operator $\mathrm{Re}\Pi(\omega, q)$. Since the latter is finite at $\omega = 0$, these contributions are as singular as AL terms. These technicalities will be explained in great details in the following section.

3.3 Fluctuation-induced conductivity near the quantum critical point

We approach the problem of transport in the in-plane magnetic field close to the superconducting transition based on the diagrammatic perturbation theory. Note that the technique based on the time-dependent Ginzburg-Landau formalism applied for studying transport near QCP [117, 118] accounts correctly only for the classical part of AL-type contribution to the conductivity, but it misses completely the quantum zero-temperature corrections. A microscopic approach takes care of all the contributions including the DOS part, resulting from the depletion of the normal state density of states by superconducting fluctuations, and also the MT interference term [110–112]. In fact, at $T = 0$, where the corrections come from purely quantum fluctuations, these effects turn out to be of the dominant nature. In calculations $T \ll \{E_z, \Delta\} \ll \tau^{-1} \ll \varepsilon_F$, these conditions are satisfied in many experiments [94, 101].

Our starting point is the current-current response kernel which can be conveniently presented as a sum of three contributions $K = K^{AL} + K^{MT} + K^{DOS}$. Within this section we will be discussing only longitudinal electrical transport so the subscript K_{xx} is suppressed in all the expressions for brevity. The general expression for the AL term reads

$$K^{AL}(\Omega_n) = -e^2 T \sum_{q,\omega_k} \mathcal{B}^2(\omega_k, \Omega_n, q)\mathcal{L}(\omega_k, q)\mathcal{L}(\omega_k + \Omega_n, q), \tag{3.6}$$

where $\omega_k = 2\pi kT$. Notice here the factor of 4 difference compared to the earlier expression Eq. (2.39). This is due to the fact that, in the finite in-plane magnetic field, different spin projections $\sigma = \pm$ contribute unevenly to the current vertex $\mathcal{B}$. It reads explicitly now as follows

$$\mathcal{B}(\omega_k,\Omega_n,q)=T\sum_{\sigma,\varepsilon_m}\lambda^\sigma(\varepsilon_{m+n},\omega_k-\varepsilon_m,q)\lambda^\sigma(\varepsilon_n,\omega_k-\varepsilon_n,q)J^\sigma_{AL},\tag{3.7}$$

$$J^\sigma_{AL}=\sum_p v_p\mathcal{G}^\sigma(\varepsilon_{n+m},p)\mathcal{G}^\sigma(\varepsilon_n,p)\mathcal{G}^{-\sigma}(-\varepsilon_n+\omega_k,-p+q),\tag{3.8}$$

with the impurity ladders

$$\lambda^\sigma(\varepsilon_n,\varepsilon_m,q)=\frac{\theta(-\varepsilon_n\varepsilon_m)}{\tau[Dq^2+|\varepsilon_n-\varepsilon_m|-i\sigma E_z\mathrm{sgn}(\varepsilon_n-\varepsilon_m)]},\tag{3.9}$$

and an integral over the block of three Green's functions with $\mathcal{G}^\sigma_{\varepsilon_n,p}=(i\varepsilon_n-\xi_p+\sigma E_z/2+i\mathrm{sgn}(\varepsilon_n)/2\tau)^{-1}$. Here we used notations: $\varepsilon_m=2\pi T(m+1/2)$, $\xi_p=p^2/2m-\varepsilon_F$, $v_p=\partial_p\xi_p$, $\theta(\varepsilon)$ is the step-function, and $\mathrm{sgn}(\varepsilon)$ is the sign-function. The propagator of fluctuating Cooper pairs in Eq. (3.6) is given by

$$\mathcal{L}^{-1}(\omega_k,q)=-\nu\left[\ln\frac{T}{T_{c0}}-\psi\left(\frac{1}{2}\right)+\frac{1}{2}\sum_{\sigma=\pm}\Psi^\sigma(\omega_k,q)\right],\tag{3.10}$$

$$\Psi^\sigma(\omega_k,q)=\psi\left(\frac{1}{2}+\frac{Dq^2+|\omega_k|+i\sigma E_z}{4\pi T}\right).\tag{3.11}$$

When calculating the $\mathcal{B}$-vertex one should follow a few basic steps which we already discussed in the previous Chapter: *i*) In the leading order in the transferred momentum q one can approximate $\mathcal{G}^{-\sigma}(-\varepsilon_n+\omega_k,-p+q)\approx\mathcal{G}^{-\sigma}(-\varepsilon_n+\omega_k,p)+\mathbf{v}\cdot\mathbf{q}[\mathcal{G}^\sigma(-\varepsilon_n+\omega_k,p)]^2$. *ii*) Furthermore, one can neglect Zeeman energy as compared to the inverse scattering time in the Green's functions (provided the condition $T\ll\{E_z,\Delta\}\ll\tau^{-1}\ll\varepsilon_F$ is satisfied) and then complete p integration in a standard way with density of states and angular averaging over the Fermi surface. *iii*) Next is the fermionic Matsubara ε_m sum in Eq. (3.7), which can be found in the closed form with the result

$$\mathcal{B}(\omega_k, \Omega_n, q) = \frac{\nu_d q_x D}{\Omega_n} \sum_\sigma \left[\Psi^\sigma(|\omega_k| + \Omega_n, q) - \Psi^\sigma(|\omega_k|, q)\right.$$
$$\left. + \Psi^\sigma(|\omega_{k+n}| + \Omega_n, q) - \Psi^\sigma(|\omega_{k+n}|, q)\right]. \tag{3.12}$$

iv) The remaining step of the calculation is a bosonic ω_k sum followed by an analytical continuation $i\omega_n \to \omega$. The latter is accomplished via the contour integration over the circle with two-branch cuts at $\mathrm{Im}(\omega) = 0, -\Omega_n$ where the product of propagators in Eq. (3.6) has breaks of analyticity. After the Ω-expansion of $K^R_{AL}(\Omega)$ to the linear order, one finds for the AL conductivity correction $\sigma^{AL} = \sigma^{AL}_{cl} + \sigma^{AL}_{q1} + \sigma^{AL}_{q2}$, where

$$\sigma^{AL}_{cl} = \frac{e^2}{4\pi T} \sum_q \int_{-\infty}^{+\infty} \frac{d\omega}{\sinh^2(\omega/2T)} [\mathcal{B}^{RA}(\omega, q)]^2 [\mathrm{Im}\mathcal{L}^R(\omega, q)]^2, \tag{3.13}$$

$$\sigma^{AL}_{q1} = \frac{e^2}{4\pi} \sum_q \int_0^\infty d\omega \coth\left(\frac{\omega}{2T}\right) \mathrm{Re}\left\{[B^{RA}(\omega, q)]^2 - [B^{RR}(\omega, q)]^2]\partial_\omega[\mathcal{L}^R(\omega, q)]^2\right\}, \tag{3.14}$$

$$\sigma^{AL}_{q2} = -\frac{e^2}{4\pi} \sum_q \int_{-\infty}^{+\infty} d\omega \coth\left(\frac{\omega}{2T}\right)$$
$$\times \left\{\partial_\Omega[B^{RR}(\omega, \Omega, q)]^2[\mathcal{L}^R(\omega, q)]^2 - \partial_\Omega[B^{AA}(\omega - \Omega, \Omega, q)]^2[\mathcal{L}^A(\omega, q)]^2\right.$$
$$\left. + \partial_\Omega[[B^{RA}(\omega - \Omega, \Omega), q]^2 - [B^{RA}(\omega, \Omega, q)]^2]|\mathcal{L}^R(\omega, q)|^2\right\}. \tag{3.15}$$

The superscript $R(A)$ in the vertex functions and propagators stands for the retarded (advanced) component while subscript $cl(q)$ refers to classical (quantum). This convention comes form the observation that as $T \to 0$ the classical contribution vanishes while the quantum contribution remains finite.

We turn now to the derivation of the MT contribution whose response kernel is given by

$$K^{MT}(\Omega_n) = e^2 T \sum_{\omega_k, q} \mathcal{L}(\omega_k, q) \Sigma^{MT}(\omega_k, \Omega_n, q), \tag{3.16}$$

where

$$\Sigma^{MT}(\omega_k, \Omega_n, q) = T \sum_{\sigma, \varepsilon_m} \lambda^{\sigma}(\varepsilon_{m+n}, \omega_{k-n} - \varepsilon_m, q) \lambda^{\sigma \mathrm{sgn}[\epsilon_m \epsilon_{m+n}]}(\varepsilon_m, \omega_k - \varepsilon_m, q) J_{MT} \tag{3.17}$$

$$J_{MT} = \sum_p v_p v_{q-p} \mathcal{G}^{\sigma}(\varepsilon_{m+n}, q) \mathcal{G}^{-\sigma}(\omega_{k-n} - \varepsilon_m, q-p) \mathcal{G}^{\sigma}(\varepsilon_m, p) \mathcal{G}^{-\sigma}(-\varepsilon_m + \omega_k, q-p). \tag{3.18}$$

Momentum integration in the block of Green's functions J_{MT} is done under the same approximations as in the case of the AL term described above. According to the standard convention [19] we now split the MT term into the so-called *regular* and *anomalous* contributions:

$$\Sigma^{MT(reg)}(\omega_k, \Omega_n, q) = -\frac{\nu_d D}{\Omega_n} \sum_{\sigma} \left[\Psi^{\sigma}(|\omega_k| + 2\Omega_n, q) - \Psi^{\sigma}(|\omega_k|, q) \right], \tag{3.19}$$

$$\Sigma^{MT(an)}(\omega_k, \Omega_n, q) = -\frac{\nu_d D}{2(Dq^2 + \Omega_n)} \sum_{\sigma} \left[\Psi^{\sigma}(-|\omega_k| + 2\Omega_n, q) - \Psi^{\sigma}(|\omega_k|, q) \right]. \tag{3.20}$$

After the analytical continuation these translate into the conductivity correction $\sigma^{MT} = \sigma^{MT}_{reg} + \sigma^{MT}_{an}$, where

$$\sigma^{MT}_{reg} = -\frac{e^2 \nu_d D}{8\pi^3 T^2} \sum_{\sigma q} \int_0^{\infty} d\omega \coth\left(\frac{\omega}{2T}\right) \mathrm{Im}[\mathcal{L}^R(\omega, q)[\Psi^{\sigma}(-i\omega, q)]''], \tag{3.21}$$

$$\sigma^{MT}_{an} = \frac{e^2 \nu_d D}{8\pi T} \sum_{\sigma q} \int_{-\infty}^{+\infty} \frac{d\omega}{\sinh^2(\omega/2T)} \frac{\mathcal{L}^R(\omega, q)[\Psi^{\sigma}(i\omega, q) - \Psi^{\sigma}(-i\omega, q)]}{Dq^2 + \Gamma}. \tag{3.22}$$

In order to regularize the logarithmically divergent momentum integral in the case of the anomalous contribution we have introduced a pair-breaking cutoff parameter Γ. The microscopic origin of the latter (e.g. spin-orbit scattering) will be discussed in the next section.

We finally discuss the DOS contribution to the conductivity. It is given by the similar to Eq. (3.16) expression with

$$K^{DOS}(\Omega_n) = e^2 T \sum_{\omega_k, q} \mathcal{L}(\omega_k, q) \Sigma^{DOS}(\omega_k, \Omega_n, q), \tag{3.23}$$

where

$$\Sigma^{DOS}(\omega_k, \Omega_n, q) = 2T \sum_{\sigma, \varepsilon_m} [\lambda^\sigma(\varepsilon_m, \omega_k - \varepsilon_m, q)]^2 J_{DOS}, \tag{3.24}$$

$$\begin{aligned} J_{DOS} = \sum_p v_p^2 [\mathcal{G}^\sigma(\varepsilon_m, p)]^2 \mathcal{G}^\sigma(\varepsilon_m + \Omega_n, p) [\mathcal{G}^{-\sigma}(\omega_k - \varepsilon_m, q - p) \\ + \frac{1}{2\pi\nu_d\tau} \sum_{p'} [\mathcal{G}^\sigma(\varepsilon_m, p')]^2 \mathcal{G}^{-\sigma}(\omega_k - \varepsilon_m, q - p')]. \end{aligned} \tag{3.25}$$

After completing the standard steps outlined above one arrives at the conductivity correction $\sigma^{DOS} = \sigma_{cl}^{DOS} + \sigma_q^{DOS}$ in the form

$$\sigma_{cl}^{DOS} = -\frac{e^2 \nu_d D}{16\pi^2 T^2} \sum_{\sigma q} \int_{-\infty}^{+\infty} \frac{d\omega [[\Psi^\sigma(i\omega, q)]' - [\Psi^\sigma(-i\omega, q)]']}{\sinh^2(\omega/2T)} \mathcal{L}^R(\omega, q), \tag{3.26}$$

$$\sigma_q^{DOS} = \sigma_{reg}^{MT}. \tag{3.27}$$

The equality between the two contributions in Eq. (3.27) has parallels with the original fluctuation transport considerations at $T - T_c \ll T$. In the original near–T_c problem, the typical energy of diffusing pairs $Dq^2 \sim T - T_c$ is smaller than the thermal energy of the quasiparticle $\sim T$. In our case, E_z adds to the energy of pairs making it bigger than T. Correspondingly, unlike the near–T_c case, the off-shell energy of a pair, $2\varepsilon \sim T$, falls below the pair excitation energy set by E_z. This causes a sign inversion of the energy denominator associated with the unbound intermediate state, and the correction Eq. (3.27) turns out to be positive. In general, the derived above conductivity corrections are applicable at any field H and temperature T above the transition. In the following, we discuss limiting cases of interest.

It is convenient to regroup all contributions and present the total conductivity correction as the a sum of zero-temperature ($\delta\sigma_q$) and finite-temperature ($\delta\sigma_T$) terms, namely

$$\delta\sigma(H,T) = \delta\sigma_q(H) + \delta\sigma_T(H,T). \tag{3.28}$$

The first term here is determined by the quantum AL [Eqs. (3.14)-(3.15) and DOS [see Eq. (3.27)] contributions, and also the regular part of the MT conductivity [see Eq. (3.21)]. The remaining terms define $\delta\sigma_T$. The magnitude of $\delta\sigma_q$ decreases monotonically with an increasing field. This leads to a pronounced magnetoresistance at zero temperature. At finite temperature, based on how the quantum critical point is approached, there are several regimes that show different T and H dependencies, which should be experimentally accessible. Below we focus on QCP only and extract the leading singularity in $\delta\sigma_q$ as the function of the Zeeman field. Thermal contribution $\delta\sigma_T$ and various crossover regimes will be discussed in the next section.

At zero temperature $\Psi^\sigma(\pm i\omega, q) \to \ln[(Dq^2 \pm i\omega + i\sigma E_z)/4\pi T]$ and the pair propagator can be taken in the leading pole approximation

$$\mathcal{L}^{R(A)}(\omega, q) \approx -\frac{2\Delta_0^2/\nu_d}{E_c^2 - (\omega \pm iDq^2)^2}, \tag{3.29}$$

which is obtained from Eq. (3.10) under the conditions $Dq^2 \ll \Delta_0$ and $|E_c \pm \Omega| \ll \Delta_0$. Here $\Delta_0 = \pi T_{c0}/2\gamma_E$ where $\ln\gamma_E \approx 0.57$ is the Euler constant, and $E_c = \sqrt{E_z^2 - \Delta_0^2}$. The branch cut of the propagator (due to the logarithmic structure) also contributes to $\delta\sigma_q$, but gives the subleading singularity. Within the same accuracy we compute the vertex functions:

$$[\mathcal{B}^{RR(AA)}(\omega(-\Omega), \Omega, q)]^2 = \frac{8\nu_d^2 D}{E_z^4} Dq^2(Dq^2 \mp i\omega)(Dq^2 \mp i\omega - 2i\Omega), \tag{3.30}$$

$$[\mathcal{B}^{RA(AR)}(\omega, \Omega, q)]^2 = \frac{8\nu_d^2 D}{E_z^4}(Dq^2)^2(Dq^2 - 2i\Omega). \tag{3.31}$$

Alltogether this leads to the conductivity correction near the Zeeman field-induced quantum critical point

$$\delta\sigma_q(H) = \frac{2e^2}{\pi^2} \ln\left(\frac{E_z}{E_z - \Delta_0}\right), \tag{3.32}$$

which is obtained within the logarithmic accuracy. Equation (3.32) is the main result of this section. We have checked explicitly that other contributions, such as the diffusion coefficient renormalization or the contribution with only one or no Cooperon vertex, are either small or nonsingular. Since the temperature can be set to zero in integrations over fast-fermion degrees of freedom, the additional factors of τ results in small prefactors τE_z, τDQ^2 or $\tau\Omega$.

3.4 Effects of pair-breaking scattering

In the preceding calculations we assumed that impurity scattering of electrons does not cause spin flips. There are two sources of spin relaxation of conduction electrons: localized spins (magnetic impurities) and spin-orbit (SO) scattering of electrons by nonmagnetic disorder. The latter is characterized by the scattering amplitude $iv_{so}([\mathbf{p}\times\mathbf{p}']\cdot\boldsymbol{\sigma})/p_F^2$, where $\mathbf{p}$ and $\mathbf{p}'$ are the initial and final momenta of an electron, and $\boldsymbol{\sigma}$ is the spin operator whose components are the Pauli matrices. Let us discuss the effect of SO scattering first starting with the qualitative physical picture [103]. In the absence of both, SO interactions and magnetic field two-spin states, which belong to a given orbital, have the same energy. Magnetic field split this degeneracy. It is important that the splitting energy E_z is exactly the same for all of the orbital states, which is no longer the case for finite SO interaction. Without an external magnetic field the states are still doubly degenerate due to time-reversal invariance (Kramers doublets). A magnetic field splits the Kramers doublets similar to how it splits pure spin states in the absence of SO interactions. The main difference is that this splitting is not exactly uniform anymore [119].

The spin-orbit scattering and finite thickness effects modify the fluctuation transport, due to the finite spectral weight in the particle-particle channel at zero frequency. The addition of a finite spin-orbit scattering introduces a finite lifetime Γ^{-1} to the Cooperon. At lowest temperatures the superconductivity survives if this scattering is not too strong, $\Gamma \ll E_z$ with a somewhat lower critical field. While E_z approaches the supercooling transition from above the results obtained in the previous section are expected to crossover to a different regime at $\Gamma \approx E_c$. The finite film thickness affects the crossover in a similar way. Inclusion of these effects was shown to be necessary for quantitative analysis of measurements of the density of states [102].

As was discussed early in Sec. 2.5 [see Eq. (2.25)] the Cooperon is formed by two electron Green's functions. In the absence of an external magnetic field it is convenient to classify Cooper poles by the total spin of the two electrons $\mathbf{S}_+ = (\boldsymbol{\sigma}_1 + \boldsymbol{\sigma}_2)/2$. Spin-orbit scattering does not affect the spin singlet part of the Cooperon ($\mathbf{S}_+^2 = 0$), however, this scattering leads to total spin relaxation, i.e., the triplet ($\mathbf{S}_+^2 = 2$) component of the Cooperon decays and, consequently, the pole in the ω plane is shifted from the real axis even for $q = 0$. An external magnetic field is coupled with the difference $\mathbf{S}_{+} = (\boldsymbol{\sigma}_1 + \boldsymbol{\sigma}_2)/2$ of two electron spins, and as a result we classified the Cooperon by the eigenvalue of the operator $\mathbf{S}_{-} \cdot \mathbf{E}_z$. These eigenvalues for $\mathbf{S}_{-}^2 = 2$ are $0, \pm E_z$, corresponding to $S_{-}^z = 0, \pm 1$ and 0 for $\mathbf{S}_{-}^2 = 0$. Neither of those two classifications is exact when both a magnetic field and SO scattering take place simultaneously. We assume that the SO effect is weak that allows us to evaluate the Cooperon perturbatively

$$\Pi(\omega, q) = 4\pi\nu_d T \sum_{\varepsilon_n > 0} \sum_{\sigma=\pm} \frac{1}{2\varepsilon_n + |\omega| + i\sigma E_z + Dq^2 + \Gamma_{so}}, \tag{3.33}$$

where $\Gamma_{so} = 2/3\tau_{so}$, and $\tau_{so}^{-1} = 2\pi\nu_d v_{so}^2$ is the time of the spin relaxation by SO scattering [compare Eq. (3.33) to Eq. (2.28)]. This consideration suggests that any physical mechanism of violation of either time-reversal invariance or conservation of spin will have a similar effect on a Cooperon field. In the following discussion we assume that $\Gamma = \Gamma_{so} + \Gamma_s + \Gamma_H$ is the total scattering rate that include spin-orbital, spin-flip and finite film thickness effects.

3.5 Thermomagnetic phenomena

Since the Cooperon is no longer a soft mode at $(\omega, q) \to 0$ and has a finite gap Γ, due to spin-related scattering processes, it inevitably enters into the pair propagator $\mathcal{L}(\omega, q)$, shifts its pole and ultimately changes temperature dependence of the kinetic coefficients. Thus with Eq. (3.33) at hand we have to recompute all the basic ingredients of the diagrammatic technique. Most importantly we find the generalized form of the fluctuation propagator

$$\mathcal{L}^R(\omega, q) = -\frac{2\Delta_0^2/\nu_d}{E_c^2 - 2i\Gamma(\omega + iDq^2) - (\omega + iDq^2)^2}, \tag{3.34}$$

which is different from the expression that we used before [Eq. (3.29)] in two important aspects. First is the presence of the new term in the denominator which introduces an additional scale E_c^2/Γ to the problem. Second is shifted value of the critical point $E_c = \sqrt{E_z^2 - \Delta_\Gamma^2}$ with $\Delta_\Gamma^2 = \Delta_0^2 + \Gamma^2$. Another important building block of the theory is the vertex function $\mathcal{B}$. We present only its mixed retarded-advanced component

$$[\mathcal{B}^{RA(AR)}(\omega, \Omega, q)]^2 = \frac{8\nu_d^2 D}{E_z^4}(Dq^2 + \Gamma)^2(Dq^2 - 2i\Omega), \tag{3.35}$$

which is the most relevant for the transport regime that we will specify next. The subsequent calculations will be carried out assuming $\Gamma \gg E_c$ and for temperatures not too close to the critical line $E_c^2/\Gamma \ll T \lesssim \Gamma \ll E_z$, which is quite relevant for the actual experimental realization. Under these conditions the third term in the denominator of Eq. (3.34) can be neglected so that one finds approximately

$$\mathrm{Im}\mathcal{L}^R(\omega, q) = -\frac{2\Delta_0^2}{\nu_d}\frac{2\Gamma\omega}{(E_c^2 + 2\Gamma Dq^2)^2 + 4\Gamma^2\omega^2}. \tag{3.36}$$

In order to determine $\delta\sigma_T(H, T)$ we have to reexamine all the contributions to fluctuation-induced conductivity. In the course of this analysis we found that the most singular term originates from the classical part of the AL contribution Eq. (3.13), so that in large $\delta\sigma_T(H, T)$ is governed by σ_{cl}^{AL}. To calculate this term explicitly in the above discussed regime, we introduce dimensionless variables $x = Dq^2/2T$, $y = \omega/2T$, $\gamma = \Gamma/2T$, and $\epsilon = E_c/2T$ and obtain from Eq. (3.13)

$$\delta\sigma_T(H, T) = \frac{16e^2}{\pi^2}\int_0^\infty dx \int_{-\infty}^{+\infty} \frac{dy}{\sinh^2 y}\frac{\gamma^2 y^2 x(x+\gamma)^2}{[(\epsilon^2 + 2\gamma x)^2 + 4\gamma^2 y^2]^2}, \tag{3.37}$$

where, in addition, we set $\Delta_0/E_z \to 1$ assuming that H is tuned sufficiently close to the transition line. The remaining integrations can be done with having small parameter $\epsilon^2/\gamma \ll 1$, which leads to the result

$$\delta\sigma_T(H,T) = \frac{e^2}{2\pi}\left(\frac{T\Gamma}{E_z^2}\right)\left(\frac{E_z}{E_z-\Delta_\Gamma}\right). \tag{3.38}$$

It is worth mentioning here that, unlike the quantum regime Eq. 3.32, which is logarithmically singular in $E_z-\Delta$, the magnetoresistance in the classical region is more pronounced. We have further checked that the other terms remain smaller and scale logarithmically $\propto \ln(E_z\Gamma/E_c^2)$ (see Appendices C and D for further details).

In a similar spirit we can calculate now α_{xy}. We have verified that, in the regime of classical fluctuations, the relation between current $\mathcal{B}^e$ and heat $\mathcal{B}^h$ vertices remains the same $\mathcal{B}^h = (-i\omega/2e)\mathcal{B}^e$, so that we can proceed immediately to Eq. (2.45) with the vertex and propagator taken from Eqs. (3.35) and (3.34) respectively. At the intermediate step one finds for transverse thermoelectric coefficient

$$\alpha_{xy} = \frac{512e}{\pi}\frac{L_T^2}{\ell_H^2}\int_0^\infty dx x^2\gamma^4\int_{-\infty}^{+\infty} dy\coth(y)\frac{\gamma y(\epsilon^2+2\gamma x)}{[(\epsilon^2+2\gamma x)^2+4\gamma^2y^2]^3} \tag{3.39}$$

and after final integrations

$$\alpha_{xy} = 2e\frac{L_z^2}{\ell_H^2}\left(\frac{\Gamma}{E_z-\Delta_\Gamma}\right), \tag{3.40}$$

where $L_z = \sqrt{D/E_z}$. We reiterate that this result is valid provided $E_c^2/\Gamma \ll T \lesssim \Gamma \ll E_z$ and observe that the singularity in α_{xy} is the same as in the conductivity $\delta\sigma_T$. This resembles similar situation as in the case of near T_c transport at zero field, namely identical scaling of the α and σ with the critical parameter, while the underlying physics is very different.

It should be stressed, however, that the field dependence of α_{xy} is extremely sensitive to the pair-breaking scattering. For completeness, we also analyzed behavior of α_{xy} in the limit of negligible $\Gamma \ll \max\{T, E_c\} \ll E_z$ and find dependence different than that give by Eq. (3.40). For that purpose, we use Eqs. (3.29) and (3.30) in the expression for α_{xy} defined by Eq. (2.57), which leads us to expression

$$\alpha_{xy} = \frac{256e}{\pi^2}\frac{L_T^2}{\ell_H^2}\int_0^{\infty} dx \int_{-\infty}^{+\infty} dy \coth(y)\frac{x^7 y(\epsilon^2 + x^2 - y^2)}{[(\epsilon^2 + x^2 - y^2)^2 + 4x^2y^2]^3}, \tag{3.41}$$

which is valid in the thermal region of fluctuations $T > E_c$. The double integral gives as factor of $9\pi^2/256\epsilon$. This implies that α_{xy} has square-toot singularity

$$\alpha_{xy} = 18\sqrt{2}e\frac{L_z^2}{\ell_H^2}\sqrt{\frac{E_z}{E_z - \Delta_0}}. \tag{3.42}$$

We conclude this section by briefly discussing behavior of α_{xy} in the regime when orbital effects of pair-breaking dominate over the spin-related effects. The phase diagram has been already discussed above based on Eq. (3.2), where we analyzed limiting case of classical and quantum fluctuation regimes. At a given pair-breaking strength α, superconductivity is destroyed at $T = T_c(\alpha)$ and at a given temperature T, at $\alpha = \alpha_c(T)$, obtained by solving Eq. (3.2) for T and for α, respectively. In the neighborhood of this classical transition, for $\alpha \ll T_{c0}$we can define the quantity $\epsilon_T(\alpha, T) = [T - T_c(\alpha)]/T_c(\alpha)/$ that measures the relative distance from the critical temperature $T_c(\alpha)$. Conversely, in the vicinity of the the pair-breaking quantum phase transition on can define the quantity $\epsilon_\alpha(\alpha, T) = [\alpha - \alpha_c(T)]/\alpha_c(T)$, which can be interpreted as the relative distance from the critical pair-breaking strength $\alpha_c(T)$ at a given $T \ll \alpha_{c0}$. In a parametrically broad temperature regime near the transition line (but not too close to the quantum region) it is legitimate to approximate pair-propagator and vertex function by the following simple expressions

$$\mathcal{L}^R(\omega, q) = -\frac{1}{\nu_d}\frac{1}{\ln(\alpha/\alpha_c(T)) + (Dq^2 - i\omega)/2\alpha_c(T)}, \quad \mathcal{B}_i = -\nu_d Dq_i/\alpha_c(T). \tag{3.43}$$

When combined with Eq. (2.57) this yields

$$\alpha_{xy} = \frac{2e}{\pi^2}\frac{L_T^2}{\ell_H^2}\int_0^\infty dx \int_{-\infty}^{+\infty} dy \frac{x^2 y \coth(\alpha_c y/T)(\epsilon_\alpha + x)}{[(\epsilon_\alpha + x)^2 + y^2]^3}, \tag{3.44}$$

where we introduced dimensionless variables for the momentum $x = Dq^2/2\alpha_c$ and frequency $y = \omega/2\alpha_c$. This result is valid for temperatures away from the critical region $T \gg \alpha_c$ so that it is legitimate to expand the cotangent at small argument. The double integral gives a factor $\pi T/8\alpha_c\epsilon_\alpha$ so that one arrives at

$$\alpha_{xy} = \frac{e}{4\pi}\frac{L_\alpha^2}{\ell_H^2}\frac{\alpha_c(T)}{\alpha - \alpha_c(T)}, \tag{3.45}$$

where we introduced new length-scale $L_\alpha = \sqrt{D/\alpha_c(T)}$, and also expanded the logarithm $\ln(\alpha/\alpha_c) \approx (\alpha - \alpha_c)/\alpha_c$ assuming close vicinity to the transition line.

Given the plethora of the different regimes and behaviors, it is desirable to have a systematic experimental study aimed specifically at exploring the physics of a pair-breaking phase transition in superconducting films from the measurements of the conductivity $\delta\sigma(H,T)$ and thermoelectric response α_{xy}. There have been few works using a parallel field as a control parameter to scan across the phase diagram, but they have had other goals mainly focussing on the physics of superconductor-insulator transition. To begin with, it will be useful to observe the finite temperature classical transition and verify the predictions of the fluctuation theory presented in this section in its vicinity. By slowly increasing the pair-breaking strength and lowering the temperature, one could approach the quantum phase transition. Having identified the right films, measurements of the temperature and pair-breaking parameter dependence of the conductivity, would afford an exciting possibility of discovering different regimes in the vicinity of the pair-breaking quantum phase transition. The non-monotonic magnetoresistance due to the presence of superconducting fluctuations that we find, is in stark contrast to the intuitive expectation and is a purely quantum effect. A clear experimental signature of such a characteristically quantum behavior would be an important step forward in the study of quantum phase transitions and low temperature superconductivity.

3.6 Summary

In this Chapter we studied electrical and thermal transport anomalies of low dimensional superconducting films in an external in-plane magnetic field. We concentrated on the Clogston-Chandrasekhar (CC) phase transition, i.e., the destruction of superconductivity by a magnetic field by virtue of the Zeeman splitting. As a result, a normal paramagnetic state of electrons is formed. The main conclusion we can draw from this study of the CC state is, that despite this state being normal (namely with the mean-field superconducting order parameter vanishing), it is drastically different from a usual normal metal with some attractive interaction. The latter state appears, e.g., in a superconductor at temperatures higher than the transition temperature T_c. The difference becomes apparent when one studies excited states rather than those close to the ground state. In particular, fluctuation-induced transport is dominated by the virtual excitations rather than real preformed Cooper pairs. This leads to a nontrivial magnetoresistance near QCP. The reason why the effects of superconducting fluctuations in a CC metal are dramatically enhanced, in comparison with the usual case, is the presence of the pole-like singularity in the correlation function of these fluctuations. This pole at a finite frequency appears due to the fact that the CC transition is of the first order. In contrast, the temperature-driven transition from superconductor to normal metal is of the second order, and in a usual normal state the correlator of the superconducting fluctuations is a smooth function of the frequency, i.e., any superconducting excitations decay very rapidly.

Near the QCP of the supercooling line of the phase diagram, magnetoresistance is governed by density of states and regular Maki-Thompson terms. We found complete cancellation of quantum Aslamazov-Larkin corrections, while anomalous Maki-Thomspon and classical Aslamazov-Larkin terms vanish in the zero-temperature limit. Nevertheless, the latter terms are crucially important in describing the crossover regimes at finite temperature where the sign of the magnetoresistance essentially depends on the direction at which the transition line is approached in the field-temperature plane. Surprisingly, we find that, near the transition line, scaling of the conductivity corrections is the same as the scaling of the transversal thermoelectric coefficient, which is analogous to usual transport anomalies near T_c and in the absence of the field. *A priori* this result is difficult to foresee since the mere mechanism of fluctuation corrections is different in the CC phase. The apparent universality between the singular field dependences of σ_{xx} and α_{xy} near the transition is another important observation of this study.

We close this Chapter by briefly discussing outstanding problems that remain largely unsolved, where our microscopic approach may give an opportunity to systematically study thermomagnetic phenomena in other various superconducting systems. Since the Nernst effect is highly sensitive to fluctuations, its measurements may shed light on the intimate connection between quantum criticality and unconventional superconductivity with competing or coexisting orders. Perhaps, the most interesting systems from that perspective are heavy-fermion superconductors (e.g. URu_2Si_2) and iron-pnictide superconductors (e.g. FeSe compounds).

It was recently reported [120] that the Nernst coefficient in URu_2Si_2 is anomalously enhanced as compared to the theoretically expected value of the standard Gaussian fluctuations. Moreover, contrary to the conventional wisdom, the enhancement is more significant with the reduction of the impurity scattering rate. This unconventional Nernst effect intimately reflects the highly unusual superconducting state embedded in the so-called hidden-order phase of URu_2Si_2 that appears to point to a new type of superconducting fluctuations generated by a degree of freedom which has not been hitherto taken into account. It is tempting to consider that such a degree of freedom is intimately related to the superconducting state with broken time-reversal symmetry. To properly address the data one has to seriously consider possible chiral or Berry-phase fluctuations associated with the broken time-reversal symmetry of the superconducting order parameter [121].

Our theory of Pauli limited superconductivity may be highly relevant for the study of FeSe superconductors. This is a unique solid state system that offers the possibility to enter the previously unexplored realm where the three energies, Fermi energy, superconducting gap, and Zeeman energy, become comparable, and thus access the crossover regime between the weakly coupled Bardeen-Cooper-Schrieffer (BCS) limit and the strongly coupled Bose-Einstein-condensate (BEC) limit. The results of the transport properties of FeSe near the BCS-BES crossover reveal intriguing features [122]. What is remarkable is that, for the Nernst effect, the Seebeck coefficient, the temperature derivative of the resistivity, and the Hall coefficient, all show peaks at around 20 K, which is twice as large as the critical temperature ($T_c \sim 10$ K). One of the most important subject in the BCS-BEC crossover is the debate concerning the mechanism — preformed pair or pseudogap. It is useful to recall that at the pseudogap temperatures of YBCO and $CeCoIn_5$, the Nernst effect exhibits its peak. Whether one can draw any conclusion from this similarity for FeSe systems remain to be seen. What is clear, is that theoretical input is urgently needed and so thermomagnetic transport in superconductors will continue to attract tremendous attention from researchers.

APPENDICES

Appendix A: Matsubara sums and analytical continuation

As outlined in the main text we convert the bosonic Matsubara sum into the integral

$$S(\Omega_\nu) = \frac{1}{4\pi i}\oint_C dz \coth\frac{z}{2T}\mathcal{L}(-iz)\mathcal{L}(-iz+\Omega_\nu), \tag{A.46}$$

where the contour of integration is a circle which contains two branch-cuts at Im$z = 0$ and Im$z = -\Omega_\nu$, [see Fig. (A.3)], where functions $\mathcal{L}(-iz)$ and $\mathcal{L}(-iz+\Omega_\nu)$ have breaks of analyticity respectively (q-dependence of propagators is suppressed here for brevity). We thus have explicitly

$$\begin{aligned} S(\Omega_\nu) = \frac{1}{4\pi i}\int_{-\infty}^{+\infty} dz \coth\frac{z}{2T}\mathcal{L}^R(-iz+\Omega_\nu)[\mathcal{L}^R(-iz) - \mathcal{L}^A(-iz)] + \\ \frac{1}{4\pi i}\int_{-\infty-i\Omega_\nu}^{+\infty-i\Omega_\nu} dz \coth\frac{z}{2T}\mathcal{L}^A(-iz)[\mathcal{L}^R(-iz+\Omega_\nu) - \mathcal{L}^A(-iz+\Omega_\nu)]\,. \end{aligned} \tag{A.47}$$

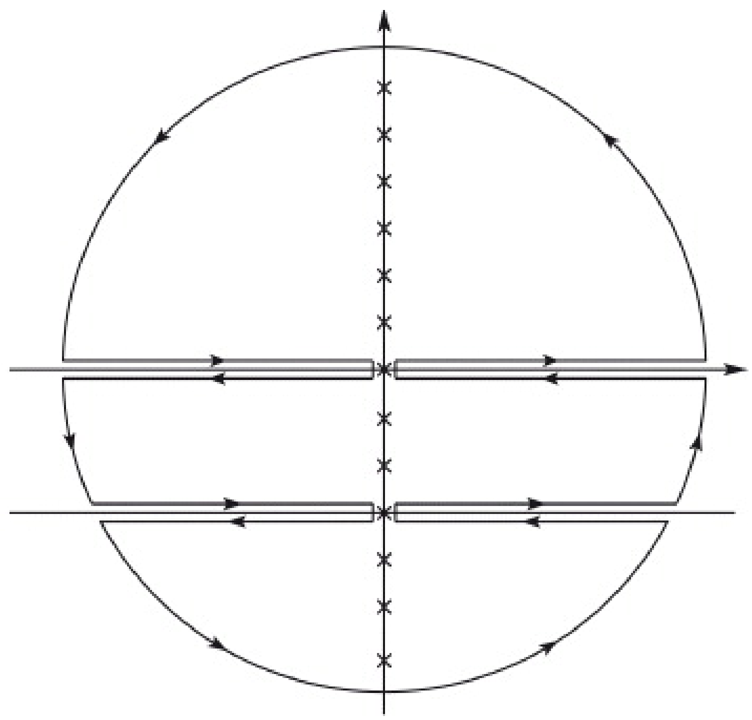

Figure A.3: Integration contour in the plane of complex frequency. The lower part of the contour corresponds to advanced-advanced products of propagators after analytical continuation. The middle section contains mixed causality components of advanced-retarded, while the upper third contains only retarded-retarded products of propagators.

In the second integral we shift variable $z + i\Omega_\nu = z'$ which gives us

$$S(\Omega_\nu) = \frac{1}{4\pi i}\int_{-\infty}^{+\infty} dz \coth\frac{z}{2T}\mathcal{L}^R(-iz+\Omega_\nu)[\mathcal{L}^R(-iz) - \mathcal{L}^A(-iz)] + \\ \frac{1}{4\pi i}\int_{-\infty}^{+\infty} dz' \coth\frac{z' - i\Omega_\nu}{2T}\mathcal{L}^A(-iz'-\Omega_\nu)[\mathcal{L}^R(-iz') - \mathcal{L}^A(-iz')]\,. \tag{A.48}$$

Taking into the account that $i\Omega_\nu$ is the periodic of cotangent $\coth\frac{z'-i\Omega_\nu}{2T} = \coth\frac{z'}{2T}$, changing back $z' \to z$ in the second integral, and taking the analytic continuation step $\Omega_\nu \to -i\Omega$, we get

$$S^R(\Omega) = \frac{1}{2\pi}\int_{-\infty}^{+\infty} dz \coth\frac{z}{2T}[\mathcal{L}^R(-iz-i\Omega,q) + \mathcal{L}^A(-iz+i\Omega,q)]\mathrm{Im}\mathcal{L}^R(-iz,q)\,. \tag{A.49}$$

Since $\mathcal{L}^R(-iz) = \mathcal{L}^A(iz)$ we get for the response kernel

$$[K^{ee}_{xx}(\Omega)]^R = \frac{2e^2}{\pi}\sum_q \mathcal{B}^2_x(q)\int_{-\infty}^{+\infty} d\omega \coth\frac{\omega}{2T}[\mathcal{L}^A(\omega+\Omega,q)+\mathcal{L}^R(\omega-\Omega,q)]\mathrm{Im}\mathcal{L}^A(\omega,q)\,. \quad \text{(A.50)}$$

We do not write imaginary i in the frequency argument of $\mathcal{L}^{R(A)}(iz)$, which is implicit in the definition. To the linear order in external frequency

$$\mathcal{L}^A(\omega+\Omega,q)+\mathcal{L}^R(\omega-\Omega,q) \approx \Omega\partial_\omega[\mathcal{L}^A(\omega,q)-\mathcal{L}^R(\omega,q)] = 2i\Omega\partial_\omega \mathrm{Im}\mathcal{L}^A(\omega,q)\,. \quad \text{(A.51)}$$

As a result the retarded component of the current-current response kernel reduces to

$$[K^{ee}_{xx}(\Omega)]^R = \frac{2i\Omega e^2}{\pi}\sum_q \mathcal{B}^2_x(q)\int_{-\infty}^{+\infty} d\omega \coth\frac{\omega}{2T}\partial_\omega\left[\mathrm{Im}\mathcal{L}^A(\omega,q)\right]^2\,, \quad \text{(A.52)}$$

which can be integrated by parts to yield Eq. (2.45).

Calculation of the Matsubara sum in the case of thermomagnetic response functions follows the same steps as above but is more involved since it contains three propagators

$$S(\Omega_m) = \frac{1}{4\pi i}\oint_C d\omega \coth\frac{\omega}{2T}(\omega+i\Omega_m/2)\left[\mathcal{L}^3(\omega,q)\mathcal{L}(\omega+i\Omega_m,q)-\mathcal{L}^3(\omega+i\Omega_m,q)\mathcal{L}(\omega,q)\right] \quad \text{(A.53)}$$

We transform this integral into a contour with branch cuts

$$\begin{aligned}S(\Omega_m) = {} & \frac{1}{4\pi i}\int_{-\infty}^{+\infty} d\omega\omega_+ \coth\frac{\omega}{2T}\left\{[\mathcal{L}^3_R(\omega,q)-\mathcal{L}^3_A(\omega,q)]\mathcal{L}_R(\omega+i\Omega,q)\right.\\ & \left.-[\mathcal{L}_R(\omega,q)-\mathcal{L}_A(\omega,q)]\mathcal{L}^3_R(\omega+i\Omega,q)\right\}\\ & +\frac{1}{4\pi i}\int_{-\infty-i\Omega}^{+\infty-i\Omega} d\omega\omega_+ \coth\frac{\omega}{2T}\left\{[\mathcal{L}_R(\omega+i\Omega,q)-\mathcal{L}_A(\omega+i\Omega,q)]\mathcal{L}^3_A(\omega,q)\right.\\ & \left.-[\mathcal{L}^3_R(\omega+i\Omega,q)-\mathcal{L}^3_A(\omega+i\Omega,q)]\mathcal{L}_A(\omega,q)\right\}\,, \end{aligned} \quad \text{(A.54)}$$

where we used notation $\omega_\pm = \omega \pm i\Omega_m/2$. In the second integral we shift $\omega + i\Omega_m \to \omega$, use the periodicity of the cotangent $\coth\frac{\omega - i\Omega_m}{2T} = \coth\frac{\omega}{2T}$, and then perform the analytic continuation $i\Omega_m \to \Omega$, which gives

$$S(\Omega) = \frac{1}{2\pi}\int_{-\infty}^{+\infty} d\omega\omega_+ \coth\frac{\omega}{2T}\left[\mathcal{L}_R(\omega+\Omega,q)\mathrm{Im}\mathcal{L}_R^3(\omega,q) - \mathcal{L}_R^3(\omega+\Omega,q)\mathrm{Im}\mathcal{L}_R(\omega,q)\right]$$
$$+\frac{1}{2\pi}\int_{-\infty}^{+\infty} d\omega\omega_- \coth\frac{\omega}{2T}\left[\mathcal{L}_A^3(\omega-\Omega,q)\mathrm{Im}\mathcal{L}_R(\omega,q) - \mathcal{L}_A(\omega-\Omega,q)\mathrm{Im}\mathcal{L}_R^3(\omega,q)\right]. \quad (A.55)$$

To the linear order in Ω, there are terms of two kind. First is the direct term proportional to Ω due to the vertex. Second, is the linear term from the expansion of propagators. We focus on the first possibility since it gives the most important contributions. We set $\Omega \to 0$ in propagators and get

$$S(\Omega) = \frac{\Omega}{4\pi}\int_{-\infty}^{+\infty} d\omega \coth\frac{\omega}{2T} \quad (A.56)$$
$$\left[\mathcal{L}_R(\omega,q)\mathrm{Im}\mathcal{L}_R^3(\omega,q) - \mathcal{L}_R^3(\omega,q)\mathrm{Im}\mathcal{L}_R(\omega,q) - \mathcal{L}_A^3(\omega,q)\mathrm{Im}\mathcal{L}_R(\omega,q) + \mathcal{L}_A(\omega,q)\mathrm{Im}\mathcal{L}_R^3(\omega,q)\right].$$

This can be rewritten as

$$S(\Omega) = \frac{\Omega}{2\pi}\int_{-\infty}^{+\infty} d\omega \coth\frac{\omega}{2T}\left[\mathrm{Re}\mathcal{L}_R(\omega,q)\mathrm{Im}\mathcal{L}_R^3(\omega,q) - \mathrm{Re}\mathcal{L}_R^3(\omega,q)\mathrm{Im}\mathcal{L}_R(\omega,q)\right], \quad (A.57)$$

or equivalently

$$S(\Omega) = \frac{\Omega}{\pi}\int_{-\infty}^{+\infty} d\omega \coth\frac{\omega}{2T}\left\{[\mathrm{Re}\mathcal{L}_R(\omega,q)]^3\mathrm{Im}\mathcal{L}_R(\omega,q) + \mathrm{Re}\mathcal{L}_R(\omega,q)[\mathrm{Im}\mathcal{L}_R(\omega,q)]^3\right\}, \quad (A.58)$$

which eventually translates into Eq. (2.57).

Appendix B:

Seebeck (α_{xx}) and Hall (σ_{xy}) coefficients near T_c

The Aslamazov-Larkin contribution to the diagonal (Seebeck) thermoelectric coefficient is found from the mixed electric-heat currents Kubo response function

$$\alpha_{xx}^{AL} = -\frac{1}{T}\lim_{\Omega\to 0}\frac{1}{\Omega}\mathrm{Im}[K_{xx}^{eh}(\Omega)]^R\,, \quad K_{xx}^{eh}(\Omega_\nu) = 2ieT\sum_{q\omega}\omega_n\mathcal{B}_x^2(q)\mathcal{L}(\omega_n,q)\mathcal{L}(\omega_n+\Omega_\nu,q). \tag{B.59}$$

Summation over the Matsubara frequency ω_n and analytical continuation follows the same way as in the case of the conductivity calculation, and we obtain

$$\alpha_{xx}^{AL} = \frac{e}{2\pi T^2}\sum_q \mathcal{B}_x^2(q)\int_{-\infty}^{+\infty}\frac{\omega d\omega}{\sinh^2(\omega/2T)}[\mathrm{Im}\mathcal{L}^R(\omega,q)]^2\,. \tag{B.60}$$

Without particle-hole asymmetry, α_{xx} is zero. Indeed, $[\mathrm{Im}\mathcal{L}^R]^2$ is even in frequency while the rest of the integrand is odd. We have to use the generalized form of the pair propagator that explicitly accounts for the particle-hole asymmetry factor Υ_ω, which is essentially dictated by gauge invariance [123]

$$\mathcal{L}(\omega_m, q) = -\frac{1}{\nu_d}\frac{1}{\pi Dq^2/8T + \epsilon + \pi|\omega_m|/8T + \Upsilon_\omega}, \quad \Upsilon_\omega = \frac{i\omega_m}{2T_c}\frac{\partial T_c}{\partial\varepsilon_F}\,. \tag{B.61}$$

Expanding $\mathcal{L}^R$ to the leading linear in Υ_ω order, $\mathrm{Im}\mathcal{L}^R = \mathrm{Im}\mathcal{L}^R|_{\Upsilon=0} + \Upsilon_\omega\partial_\epsilon\mathrm{Im}\mathcal{L}^R|_{\Upsilon=0}$ produces

$$\alpha_{xx}^{AL} = \frac{e}{\pi T^2}\sum_q \mathcal{B}_x^2(q)\int_{-\infty}^{+\infty}\frac{\omega\Upsilon_\omega d\omega}{\sinh^2(\omega/2T)}\mathrm{Im}\mathcal{L}^R(q,\omega)\partial_\epsilon\mathrm{Im}\mathcal{L}^R(\omega,q), \tag{B.62}$$

where now both propagators are taken at $\Upsilon_\omega = 0$. After introducing dimensionless variables, at the intermediate step, one has

$$\alpha_{xx}^{AL} = \frac{8Te}{\pi^3\varepsilon_F}\frac{d\ln T_c}{d\ln\varepsilon_F}\int_0^{x_{max}}dx\int_{-\infty}^{+\infty}dy\frac{xy^2(x+\epsilon)}{[(\epsilon+x)^2+y^2]^3}\,. \tag{B.63}$$

Logarithmically divergent momentum (x-integration) has to be regularized so that we introduced upper cut-off $x_{max} \simeq 1/\epsilon$ (in the original notations this corresponds to $(\xi_T q_{max})^2 \simeq 1$. This choice is natural since $\mathcal{L}^R$, in the form we use, was obtained from the expansion of the digamma function which works only as long as $\max\{Dq^2,\omega\} < T$). After the final integrations one finds

$$\alpha_{xx}^{AL} = \frac{2Te}{\pi^2 E_F}\frac{d\ln T_c}{d\ln E_F}\ln\left(\frac{T_c}{T-T_c}\right)\,. \tag{B.64}$$

In order to calculate the Hall coefficient, we need to know the transversal component of the current-current correlation function $K_{xy}^{ee} \sim \sum \mathcal{B}_x\mathcal{B}_y\mathcal{L}\mathcal{L}$. In the presence of Landau quantization the vertex in real space becomes an operator

$$\hat{\mathcal{B}}_i = -2\nu_d\eta(-i\nabla_i + 2eA_i), \tag{B.65}$$

where we choose the vector potential in the Landau gauge $A = (0, Hx, 0)$. Different components of the vertex, $\hat{\mathcal{B}}_x$ and $\hat{\mathcal{B}}_y$, do not commute and the matrix elements are

$$\hat{\mathcal{B}}_{\alpha}^{nn'} = -\frac{2\sqrt{2}\nu_d\eta}{\ell_H}\begin{cases} i\langle n|\hat{a} - \hat{a}^{\dagger}|n'\rangle & \alpha = x \\ \langle n|\hat{a} + \hat{a}^{\dagger}|n'\rangle & \alpha = y \end{cases}, \tag{B.66}$$

where $\hat{a}, \hat{a}^{\dagger}$ are oscillator operators. Recalling that $\langle n|\hat{a}|n'\rangle = \langle n'|\hat{a}^{\dagger}|n\rangle = \sqrt{n}\delta_{n,n'+1}$, we see that only transitions between nearest Landau levels $n \to n \pm 1$ are allowed. With this at hand we find for the Matsubara response kernel [123]

$$K_{xy}^{ee}(\Omega) = \frac{(4e\nu_d\eta)^2}{8\pi\ell_H^4}T\sum_{\omega}\sum_{n=0}^{\infty}(n-1)[\mathcal{L}_{n+1}(\omega, q)\mathcal{L}_n(\omega-\Omega, q)-\mathcal{L}_n(\omega, q)\mathcal{L}_{n+1}(\omega-\Omega, q)]\,. \tag{B.67}$$

After analytic continuation one gets

$$\sigma_{xy}^{AL} = -\frac{(4e\nu_d\eta)^2}{4\pi^2\ell_H^4}\sum_{n=0}^{\infty}(n+1)\int_{-\infty}^{+\infty}d\omega\coth\left(\frac{\omega}{2T}\right)$$
$$\left[\mathrm{Im}\mathcal{L}_n^R(\omega, q)\partial_{\omega}\mathrm{Re}\mathcal{L}_{n+1}^R(\omega, q) - \mathrm{Im}\mathcal{L}_{n+1}^R(\omega, q)\partial_{\omega}\mathrm{Re}\mathcal{L}_n^R(\omega, q)\right]. \tag{B.68}$$

In the weak field limit, one needs only the first term in the expansion in powers of $1/n$ and then substitute integral for the n summation $(1/\ell_H)^2\sum_n \to \sum_q$. Taking into account $\partial_n\mathcal{L}_n = 2\nu(\eta/\ell_H^2)\mathcal{L}_n^2$ and, after some algebra, we find

$$\sigma_{xy}^{AL} = -\frac{(4e\eta)^2\nu_d^3\eta}{3\pi T\ell_H^2}\sum_q q^2\int_{-\infty}^{+\infty}\frac{d\omega}{\sinh^2(\omega/2T)}[\mathrm{Im}\mathcal{L}^R(\omega, q)]^3, \tag{B.69}$$

where we also used integration by parts with respect to the energy variable. Since $[\mathrm{Im}\mathcal{L}^R(\omega, q)]^3$ is odd in energy without particle-hole asymmetry, σ_{xy}^{AL} vanishes in this case. Expanding to the lowest non-vanishing order we get

$$\sigma_{xy}^{AL} = \frac{(4e\eta)^2\nu_d^4\eta}{2\pi T\ell_H^2}\frac{\partial\ln T_c}{\partial\varepsilon_F}\sum_q q^2\int_{-\infty}^{+\infty}\frac{\omega d\omega}{\sinh^2(\omega/2T)}[\mathrm{Im}\mathcal{L}^R(\omega,q)]^2\mathrm{Im}[\mathcal{L}^R(\omega,q)]^2. \tag{B.70}$$

Introducing, as usual, dimensionless variables and using integrals $\int_0^{+\infty} xdx/(x+1)^4 = 1/6$ and $\int_{-\infty}^{+\infty} y^2dy/(y^2+1)^4 = \pi/16$ we finally get

$$\sigma_{xy}^{AL} = \frac{e^2}{48}(\omega_c\tau)\frac{\partial\ln T_c}{\partial\ln\varepsilon_F}\left(\frac{T_c}{T-T_c}\right)^2, \tag{B.71}$$

where $\omega_c = eH/m$ is cyclotron frequency.

Appendix C:

Quantum Aslamazov-Larkin terms

Within this section we analyze more carefully the unconventional AL terms in the quantum limit $T \to 0$. We start from Eq. (3.14) and obtain, in the dimensionless variables of the main text

$$\sigma_{q1}^{AL} = -\frac{e^2}{2\pi^2} \int_{-\infty}^{+\infty} dy \coth(\pi y) \int_0^\infty dx \left[(-iy)(-iy + 2x) x \frac{\partial}{\partial y} \left(\frac{-2}{\epsilon^2 + (x - iy)^2} \right)^2 + c.c. \right]. \tag{B.72}$$

Here *c.c.* stands for the complex conjugate term. In this expression we can replace the integrand with $\int_{-\infty}^{+\infty} dy \coth(\pi y)[\ldots] \to 2 \int_0^\infty dy \coth(\pi y) \mathrm{Re}[\ldots]$. At $\epsilon \gg 1$, $\coth \pi y \approx 1$, and using the integral

$$4 \int_0^\infty dy (-iy)(-iy + 2x) \partial_y \frac{4}{[\epsilon^2 + (x - iy)^2]^2} = -\frac{16}{x^2 + \epsilon^2}, \tag{B.73}$$

we obtain

$$\sigma_{q1}^{AL} = \frac{8e^2}{\pi^2} \ln \frac{E_z}{E_c} \simeq \frac{8e^2}{\pi^2} \ln \sqrt{\frac{E_z}{2(E_z - \Delta_0)}}. \tag{B.74}$$

In the opposite limit, $\epsilon \ll 1$, the expansion of $\coth(\pi y) \approx 1/\pi y$ gives the vanishing real part of the integrand. We therefore conclude that this contribution is not singular in the high temperature limit when $T \gg E_c$.

The second type of unconventional AL corrections comes from differentiating the triangular vertices $\mathcal{B}$ instead of the propagators. In the dimensionless notations, Eq. (3.15) can be reduced to the form

$$\sigma_{q2}^{AL} = \frac{ie^2}{\pi^2} \int_{-\infty}^{+\infty} dy \coth \pi y \int_0^{\infty} dx x \left[(-iy + x)[l^R(x,y)]^2 - (iy + x)[l^A(x,y)]^2 \right], \quad \text{(B.75)}$$

where

$$l^{R(A)}(x,y) = -\frac{2}{\epsilon^2 + (x \mp iy)^2}. \quad \text{(B.76)}$$

In the low-temperature, quantum limit $T \ll E_c$, one uses the integral

$$\int_0^{\infty} dy \frac{4(-iy + x)}{[\epsilon^2 + (x - iy)^2]^2} = \frac{2i}{\epsilon^2 + x^2} \quad \text{(B.77)}$$

to obtain

$$\sigma_{q2}^{AL} = -\frac{8e^2}{\pi} \ln \frac{E_z}{E_c}. \quad \text{(B.78)}$$

In the opposite limit, at higher temperatures away from the critical point, $\sigma_{q2}^{AL} = -2e^2/\pi\epsilon$. Comparing σ_{q1}^{AL} and σ_{q2}^{AL} in the quantum limit $T \to 0$, we observe acomplete cancellation effect, namely AL terms have no divergent, singular correction in E_z/E_c near QCP. As discussed in the main text, magnetoresistance $\delta\sigma_q(H)$ is determined by DOS and MT contributions.

Appendix D:

Anomalous Maki-Thompson terms

In the main text we introduced the pair-breaking (dephasing) parameter Γ in order to regularize the anomalous MT term. As discussed in details in Sec. (3.4), Γ naturally appears as a result of spin-flip scattering. We thus concentrate on the Γ-dependence of the anomalous MT term from Eq. (3.22) in various temperature regimes. In the dimensionless notations, Eq. (3.22) reduces to

$$\sigma_{an}^{MT} = \frac{e^2}{\pi}\int_{-\infty}^{+\infty}\frac{dy}{\sinh^2(\pi y)}\int_0^{\infty} dx \frac{1}{(\Gamma/2\pi T + x)}\frac{(xy)^2}{[y^2-(\epsilon - ix)^2][y^2-(\epsilon+ix)^2]}. \tag{B.79}$$

In the high temperature limit $\epsilon \ll 1$ (or equivalently in original notations $T \gg E_c$)

$$\sigma_{an}^{MT} = \frac{e^2}{\pi^3}\int_{-\infty}^{+\infty} dy \int_0^{\infty} dx \frac{1}{(\Gamma/2\pi T + x)}\frac{x^2}{[y^2-(\epsilon - ix)^2][y^2-(\epsilon+ix)^2]}, \tag{B.80}$$

which eventually reduces to

$$\sigma_{an}^{MT} = \frac{e^2}{2\pi^2}\int_0^{\infty} dx \frac{1}{(\Gamma/2\pi T + x)}\frac{x}{x^2+\epsilon^2} = \frac{e^2}{2\pi^2}\frac{\pi\epsilon/2 - (\Gamma/2\pi T)\ln(2\pi T\epsilon/\Gamma)}{(\Gamma/2\pi T)^2+\epsilon^2}. \tag{B.81}$$

From this expression we can extract various limiting cases. For $\Gamma/2 < 2\pi E_c < T$, which is possible if $\Gamma/2 < T$, one finds $\sigma_{an}^{MT} = e^2/4\pi\epsilon$. Alternatively, for $2\pi E_c < \Gamma/2 < T$, which is possible if $\Gamma/2 < T$, or for $2\pi E_c < T < \Gamma/2$, which is possible if $\Gamma/2 > T$, one finds $\sigma_{an}^{MT} = (e^2/\pi)(T/\Gamma)\ln(\Gamma/E_c)$.

We proceed with the low temperature limit $\epsilon \gg 1$ (or equivalently $T \ll E_c$). In this case we have

$$\sigma_{an}^{MT} = \frac{e^2}{\pi}\int_{-\infty}^{+\infty}\frac{dyy^2}{\sinh^2(\pi y)}\int_0^\infty dx\frac{1}{(\Gamma/2\pi T + x)}\frac{x^2}{[\epsilon^2 + x^2]^2}. \tag{B.82}$$

At $T < E_c < \Gamma$,

$$\sigma_{an}^{MT} = \frac{e^2}{3\pi^2}\frac{2\pi T}{\Gamma}\int_0^\infty \frac{x^2dx}{(x^2+\epsilon^2)^2} = \frac{e^2}{12\pi\epsilon}\frac{2\pi T}{\Gamma}. \tag{B.83}$$

Alternatively, at $T < \Gamma < E_c$ or $\Gamma < T < E_c$,

$$\sigma_{an}^{MT} = \frac{e^2}{3\pi^2}\int_0^\infty \frac{xdx}{(x^2+\epsilon^2)^2} = \frac{e^2}{6\pi^2\epsilon^2}, \tag{B.84}$$

and consequently, the anomalous MT term has no singular contributions near QCP. The logarithmically divergent correction declared in Eq. (3.32) of the main text originates from the regular part of the MT term. Indeed, from Eq. (3.21) we obtain

$$\sigma_{reg}^{MT} = \frac{4e^2}{\pi^2}\int_0^\infty dx\int_0^\infty dy\coth(\pi y)\frac{xy}{[(y+\epsilon)^2+x^2][(y-\epsilon)^2+x^2]}. \tag{B.85}$$

At high temperatures $T \gg E_c$,

$$\sigma_{reg}^{MT} = \frac{4e^2}{\pi^3}\int_0^\infty dx\int_0^\infty dy\frac{x}{[(y+\epsilon)^2+x^2][(y-\epsilon)^2+x^2]} = \frac{e^2}{2\pi\epsilon}, \tag{B.86}$$

while at low temperatures $T \ll E_c$, near QCP ,

$$\sigma_{reg}^{MT} = \frac{4e^2}{\pi^2} \int_0^\infty dx \int_0^\infty dy \frac{xy}{[(y+\epsilon)^2 + x^2][(y-\epsilon)^2 + x^2]} \approx \frac{2e^2}{\pi^2} \ln(E_z/E_c). \tag{B.87}$$

BIBLIOGRAPHY

BIBLIOGRAPHY

[1] L. D. Landau, JETP **7**, 19 (1937)

[2] L. P. Kadanoff, Physics **2**, 263 (1966).

[3] A. Z. Patashinskii and V. L. Pokrovsky, **50**, 439 (1966).

[4] V. N. Gribov and A. A. Migdal, JETP **55**, 1498 (1968).

[5] A. M. Polyakov, JETP **55**, 1026 (1968).

[6] B. I. Halperin and P. C. Hohenberg, Phys. Rev. **168**, 898 (1969).

[7] K. G. Wilson, Phys. Rev. B **4** 3174 (1971); *ibid* **4**, 3184 (1971).

[8] V. L. Ginzburg, Sov. Solid State Phys. **2**, 61 (1960).

[9] J. Bardeen, L. N. Cooper, and J. R. Schrieffer, Phys. Rev. **108**, 1175 (1957).

[10] L. G. Aslamazov and A. I. Larkin, Phys. Lett. **26A**, 238 (1968).

[11] K. Maki, Prog. Theor. Phys. **39**, 897 (1968).

[12] R. S. Thompson, Phys. Rev. B **1**, 327 (1970).

[13] R. E. Glover, Phys. Rev. Lett. **A25**, 542 (1697).

[14] W. A. Little, Phys. Rev. **156**, 396 (1967).

[15] J. S. Langer and V. Ambegaokar, Phys. Rev. **164**, 498510 (1967).

[16] D. E. McCumber and B. I. Halperin, Phys. Rev. B **1**, 1054 (1970).

[17] N. Giordano, Phys. Rev. Lett. **61**, 2137 (1988).

[18] E. Abrahams, M. Redi, and J. W. F. Woo, Phys. Rev. B **1**, 208 (1970).

[19] A. I. Larkin and A. Varlamov, *Theory of fluctuations in superconductors* (Clarendon Press, Oxford, 2005).

[20] B. L. Al'tshuler, JETP Lett. **41**, 648 (1985).

[21] B. L. Al'tshuler and D. E. Khmel'nitskii, JETP Lett. **42**, 359 (1986).

[22] P. A. Lee and A. D. Stone, Phys. Rev. Lett. **55**, 1622 (1985).

[23] P. A. Lee, A. D. Stone, and H. Fukuyama, Phys. Rev. B **35**, 1039 (1987).

[24] G. D. Mahan, *Many-Particle Physics*, (Kluwer Academic, 2000).

[25] I. L. Aleiner and Ya. M. Blanter, Phys. Rev. B **65**, 115317 (2002).

[26] B. L. Altshuler and B. I. Shklovskii, Sov. Phys. JETP **64**, 127 (1986).

[27] M. L. Mehta, *Random Matrices*, (Elsevier, 2004).

[28] S. G. den Hartog, C. M. A. Kapteyn, B. J. van Wees, T. M. Klapwijk, W. van der Graaf, and G. Borghs, Phys. Rev. Lett. **76**, 4592 (1996).

[29] K. Hecker, H. Hegger, A. Altland, and K. Fiegle, Phys. Rev. Lett. **79**, 1547 (1997).

[30] P. W. Brouwer and C. W. J. Beenakker, Phys. Rev. B **52**, 16772 (1995).

[31] A. Altland and M. R. Zirnbauer, Phys. Rev. B **55**, 1142 (1997).

[32] T. T. Heikkila, M. M. Salomaa, and C. J. Lambert, Phys. Rev. B **60**, 9291 (1999).

[33] A. Frydman, E. P. Price, and R. C. Dynes, Solid State Comm. **106**, 715 (1998).

[34] A. Frydman, E. P. Price, and R. C. Dynes, Phys. Uspekhi **41**, 220 (1998).

[35] Yu. Zadorozhny, D. R. Herman, and Y. Liu, Phys. Rev. B **63**, 1444521 (2001).

[36] A. V. Herzog, P. Xiong, and R. C. Dynes, Phys. Rev. B **58**, 14199 (1998).

[37] A. Johansson, G. Sambandamurthy, D. Shahar, N. Jacobson, R. Tenne, Phys. Rev. Lett. **95**, 116805 (2005).

[38] B. L. Altshuler and B. Z. Spivak, Sov. Phys. JETP **65**, 343 (1987).

[39] B. Z. Spivak and A. Yu. Zyuzin, JETP Lett. **47**, 267 (1988).

[40] C. W. J. Beenakker, Phys. Rev. Lett. **67**, 3836 (1991).

[41] T. Micklitz, Phys. Rev. B **75**, 144509 (2007).

[42] M. Houzet and M. A. Skvortsov, Phys. Rev. B **77**, 024525 (2008).

[43] B. Spivak and F. Zhou, Phys. Rev. Lett. **74**, 2800 (1995).

[44] V. M. Galitski and A. I. Larkin, Phys. Rev. Lett. **87**, 087001 (2001).

[45] M. A. Skvortsov and M. V. Feigel'man, Phys. Rev. Lett. **95**, 057002 (2005).

[46] F. Zhou and B. Spivak, Phys. Rev. Lett. **80**, 5647 (1998).

[47] A. Lamacraft, F. M. Marchetti, J. S. Meyer, R. S. Moir, and B. D. Simons, J. Phys. A **37**, L447 (2004).

[48] F.-von Oppen and E. K. Riedel, Phys. Rev. B **46**, 3203(R) (1992).

[49] A. I. Buzdin and A. A. Varlamov, Phys. Rev. Lett. **89**, 076601 (2002).

[50] G. Schwiete and Y. Oreg, Phys. Rev. Lett. **103**, 037001 (2009); Phys. Rev. B **82**, 214514 (2010).

[51] O. Entin-Wohlamn, H. Bary-Soroker, A. Aharony, Y. Imry, and J. G. E. Harris, Phys. Rev. B **84**, 184519 (2011).

[52] J. A. Melsen, P. W. Brouwer, K. M. Frahm and C. W. J. Beenakker, Europhys. Lett. **35**, 7 (1996).

[53] A. Altland, B. D. Simons, and D. Taras-Semchuk, JETP Lett. **67**, 22 (1998); Adv. Phys. **49**, 321 (2000).

[54] M. G. Vavilov, P. W. Brouwer, V. Ambegaokar and C. W. J. Beenakker, Phys. Rev. Lett. **86**, 874877 (2001).

[55] P. M. Ostrovsky, M. A. Skvortsov, and M. V. Feigel'man Phys. Rev. Lett. **87**, 027002 (2001).

[56] J. S. Meyer and B. D. Simons, Phys. Rev. B **64**, 134516 (2001).

[57] B. Z. Spivak and A. Yu. Zyuzin, Europhys. Lett. **8**, 669 (1989).

[58] F. Zhou and C. Biagini, Phys. Rev. Lett. **81**, 4724 (1998).

[59] A. Pourret, H. Aubin, J. Lesueur, C. A. Marrache-Kikuchi, L. Berge, L. Dumoulin, and K. Behnia, Nat. Phys. **2**, 683 (2006); Phys. Rev. B **76**, 214504 (2007).

[60] A. Pourret, P. Spathis, H. Aubin, and K. Behnia, New J. Phys. **11**, 055071 (2009).

[61] Z. A. Xu, N. P. Ong, Y. Wang, T. Kakeshita, and S. Uchida, Nature (London) **406**, 486 (2000).

[62] Y. Wang, Z. A. Xu, T. Kakeshita, S. Uchida, S. Ono, Y. Ando, and N. P. Ong, Phys. Rev. B **64**, 224519 (2001).

[63] Y. Wang, N. P. Ong, Z. A. Xu, T. Kakeshita, S. Uchida, D. A. Bonn, R. Liang, and W. N. Hardy, Phys. Rev. Lett. **88**, 257003 (2002).

[64] C. Capan, K. Behnia, J. Hinderer, A. G. M. Jansen, W. Lang, C. Marcenat, C. Marin, and J. Flouquet, Phys. Rev. Lett. **88**, 056601 (2002).

[65] H. H. Wen, Z. Y. Liu, Z. A. Xu, Z. Y. Weng, F. Zhou, and Z. X. Zhao, Europhys. Lett. **63**, 583 (2003).

[66] Z. A. Xu, J. Q. Shen, S. R. Zhao, Y. J. Zhang, and C. K. Ong, Phys. Rev. B **72**, 144527 (2005).

[67] Y. Wang, L. Li, and N. P. Ong, Phys. Rev. B **73**, 024510 (2006).

[68] P. Li and R. L. Greene, Phys. Rev. B **76**, 174512 (2007).

[69] F. F. Tafti, F. Laliberte, M. Dion, J. Gaudet, P. Fournier, and L. Taillefer, Phys. Rev. B **90**, (2014).

[70] R. Bel, H. Jin, K. Behnia, J. Glouguet, and P. Lejay, Phys. Rev. B **70**, 220501(R) (2004).

[71] R. Bel, K. Behnia, Y. Nakajima, K. Izawa, Y. Matsuda, H. Shishido, R. Settai, and Y. Onuki, Phys. Rev. Lett. **92**, 217002 (2004).

[72] Y. Onose, L. Li, C. Petrovic, and N. P. Ong, Europhys. Lett. **79**, 17006 (2007).

[73] I. Ussishkin, S. L. Sondhi, and D. A. Huse, Phys. Rev. Lett. **89**, 287001 (2002).

[74] I. Ussishkin, Phys. Rev. B **68**, 024517 (2003).

[75] V. Oganesyan and I. Ussishkin, Phys. Rev. B **70**, 054503 (2004).

[76] S. A. Hartnoll, P. K. Kovtun, M. Muller, and S. Sachdev, Phys. Rev. B **76**, 144502 (2007).

[77] D. Podolsky, S. Raghu, and A. Vishwanath, Phys. Rev. Lett. **99**, 117004 (2007).

[78] S. Raghu, D. Podolsky, A. Vishwanath, and D. A. Huse, Phys. Rev. B **78**, 184520 (2008).

[79] A. Sergeev, M. Yu. Reizer, and V. Mitin, Phys. Rev. B **77**, 064501 (2008).

[80] M. N. Serbyn, M. A. Skvortsov, A. A. Varlamov, and V. Galitski, Phys. Rev. Lett. **102**, 067001 (2009).

[81] K. Michaeli and A. M. Finkel'stein, Europhys. Lett. **86**, 27007 (2009); Phys. Rev. B **80**, 214516 (2009).

[82] I. Martin and C. Panagopoulos, Europhys. Lett. **91**, 67001 (2010).

[83] A. Levchenko, M. R. Norman, and A. A. Varlamov, Phys. Rev. B **83**, 020506(R) (2011).

[84] N. R. Cooper, B. I. Halperin, and I. M. Ruzin, Phys. Rev. B **55**, 2344 (1997).

[85] L. G. Aslamazov and A. I. Larkin, JETP **40**, 321 (1975).

[86] S. Hikami, Phys. Rev. B **24**, 2671 (1981).

[87] I. V. Lerner, A. A. Varlamov, and V. M. Vinokur, Phys. Rev. Lett. **100**, 117003 (2008).

[88] J. Mosqueira, J. D. Dancausa, and F. Vidal, Phys. Rev. B **84**, 174518 (2011).

[89] S. Goswami, C. Siegert, M. Pepper, I. Farrer, D. A. Ritchie, and A. Ghosh, Phys. Rev. B **83**, 073302 (2011).

[90] A. M. Clogston, Phys. Rev. Lett. **9**, 266 (1962).

[91] B. S. Chandrasekhar, Appl. Phys. Lett. **1**, 7 (1962).

[92] X. S. Wu, P. W. Adams, Phys. Rev. Lett. **73**, 1412 (1994).

[93] P. W. Adams, P. Herron, and E. I. Meletis, Phys. Rev. B **58**, R2952 (1998).

[94] V. Yu. Butko, P. W. Adams, and I. L. Aleiner, Phys. Rev. Lett. **82**, 4284 (1999).

[95] T. Suzuki, Y. Seguchi and T. Tsuboi, J. Phys. Soc. Jpn. **69**, 1462 (2000).

[96] X. S. Wu, P. W. Adams, and G. Catelani, Phys. Rev. B. **74**, 144519 (2006).

[97] P. Fulde and R. A. Ferrel, Phys. Rev. **135**, 550 (1964);

[98] A. I. Larkin and Yu. N. Ovchinnikov, Sov. Phys. JETP **20**, 762 (1965).

[99] P. Fulde, Adv. Phys **22**, 667 (1973).

[100] A. A. Abrikosov and L. P. Gor'kov, Sov. Phys. JETP **12**, 1243 (1961).

[101] P. W. Adams, Phys. Rev. Lett. **92**, 067003 (2004).

[102] G. Catelani, Y. M. Xiong, X. S. Wu, and P. W. Adams, Phys. Rev. B **80**, 054512 (2009).

[103] I. L. Aleiner and B. L. Altshuler, Phys. Rev. Lett. **79**, 4242 (1997)

[104] H.-Y. Kee, I. L. Aleiner, and B. L. Altshuler, Phys. Rev B **58**, 5757 (1998).

[105] G. Catelani, Phys. Rev. B **73**, 020503(R) (2006).

[106] H. J. Gardner, A. Kumar, L. Yu, P. Xiong, M. P. Warusawithana, L. Wang, O. Vafek, and D. G. Schlom, Nat. Phys. **7**, 895 (2011).

[107] K. Michaeli, A. C. Potter, P. A. Lee, Phys. Rev. Lett. **108**, 117003 (2012).

[108] V. F. Gantmakher, S. N. Ermolov, G. E. Tsydynzhapov, A. A. Zhukov, T. I. Baturina, JETP Lett. **77**, 424 (2003); JETP Lett. **71**, 473 (2000).

[109] K. A. Parendo, L. M. Hernandez, A. Bhattacharya, and A. M. Goldman, Phys. Rev. B **70**, 212510 (2004).

[110] V. M. Galitski and A. I. Larkin, Phys. Rev. B **63**, 174506 (2001).

[111] A. V. Lopatin, N. Shah, and V. M. Vinokur, Phys. Rev. Lett. **94**, 037003 (2005).

[112] A. Glatz, A. A. Varlamov, and V. M. Vinokur, Phys. Rev. B **84**, 104510 (2011).

[113] P. Fulde and K. Maki, Z. Physik **238**, 233 (1970).

[114] K. Aoi, R. Meservey and P. M. Tedrow, Phys. Rev. B **9**, 875 (1974).

[115] P. M. Tedrow and R. Meservey, Phys. Rev. B **16**, 4825 (1977).

[116] A. G. Aronov, S. Hikami, and A. I. Larkin, Phys. Rev. Lett. **62**, 965 (1989).

[117] R. Ramazashvili and P. Coleman, Phys. Rev. Lett. **79**, 3752 (1997).

[118] V. P. Mineev and M. Sigrist, Phys. Rev. B **63**, 172504 (2001).

[119] V. E. Kravtsov and M. R. Zirnbauer, Phys. Rev. B **46**, 4332 (1992).

[120] T. Yamashita, Y. Shimoyama, Y. Haga, T. D. Matsuda, E. Yamamoto, Y. Onuki, H. Sumiyoshi, S. Fujimoto, A. Levchenko, T. Shibauchi, Y. Matsuda, Preprint – arXiv:1411.1233.

[121] H. Sumiyoshi and S. Fujimoto, Preprint – arXiv:1403.3977.

[122] S. Kasahara, T. Watashige, T. Hanaguri, Y. Kohsaka, T. Yamashita, Y. Shimoyama, Y. Mizukami, R. Endo, H. Ikeda, K. Aoyama, T. Terashima, S. Uji, T. Wolf, H. v. Lohneysenn, T. Shibauchi, Y. Matsuda, Preprint – arXiv:1411.1232.

[123] A. G. Aronov, S. Hikami, and A. I. Larkin, Phys. Rev. B **51**, 3880 (1995).